

Summer 2001

Hydrographic Variability on Decadal and Interdecadal Scales in the Northern Gulf of Alaska

Nandita Sarkar
Old Dominion University

Follow this and additional works at: https://digitalcommons.odu.edu/oeas_etds



Part of the [Oceanography Commons](#)

Recommended Citation

Sarkar, Nandita. "Hydrographic Variability on Decadal and Interdecadal Scales in the Northern Gulf of Alaska" (2001). Master of Science (MS), Thesis, Ocean & Earth Sciences, Old Dominion University, DOI: 10.25777/st5t-t229
https://digitalcommons.odu.edu/oeas_etds/99

This Thesis is brought to you for free and open access by the Ocean & Earth Sciences at ODU Digital Commons. It has been accepted for inclusion in OES Theses and Dissertations by an authorized administrator of ODU Digital Commons. For more information, please contact digitalcommons@odu.edu.

HYDROGRAPHIC VARIABILITY ON DECADAL AND INTERDECADAL SCALES IN THE NORTHERN GULF OF ALASKA

by

Nandita Sarkar
Master of Science

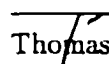
A Thesis Submitted to the Faculty of
Old Dominion University in Partial Fulfillment of the
Requirement for the Degree of

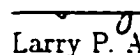
MASTER OF SCIENCE

OCEANOGRAPHY

OLD DOMINION UNIVERSITY
August, 2001

Approved by:


Thomas C. Royer (Director)


Larry P. Atkinson,


Howard J. Freeland


Chester E. Grosch

ABSTRACT

HYDROGRAPHIC VARIABILITY ON DECADAL AND INTERDECADAL SCALES IN THE NORTHERN GULF OF ALASKA

Nandita Sarkar

Old Dominion University, 2001

Director: Dr. Thomas C. Royer

The mixed layer depth (MLD) in the North Pacific is important to vertical mixing and hence the flux nutrients into the euphotic zone. A time series of hydrographic measurements, temperature and salinity versus depth, at a coastal site in the northern Gulf of Alaska is used to determine the seasonal and interannual variations in the MLD. Data from this station called GAK 1 ($59^{\circ}50.7'N$, $149^{\circ}28.0'W$) in 263 m of water begin in 1974 and end in 1998. The MLD changes seasonally from about 50 m in summer to more than 130 m in winter. These changes are in response to the seasonal variations in the wind stress, solar heating, precipitation, and freshwater discharge. The 25 years of hydrographic data allow the determination of interannual variations in the MLD. The MLD trend over this period is for a slight increase in the MLD that is not statistically significant. This is in contrast to others who found a significant shoaling of the MLD in the central region of the Gulf of Alaska (Ocean Station P, $50^{\circ}N$, $145^{\circ}W$). This difference in the response of the marine system is reasonable if one assumes that an increase in the circulation of the Alaskan Gyre will result in enhanced upwelling in the central gulf (OSP) and enhanced downwelling along the coast (GAK 1). The seasonal and interannual variations of the GAK 1 temperatures and salinities reveal 1) a possible coupling between salinity, density and freshwater discharge and 2) a strong coupling between temperature and Pacific Decadal Oscillation (PDO) and the Southern Oscillation Index (SOI). Spectral analyses of the hydrographic parameters and environmental parameters of PDO, upwelling (downwelling), freshwater

discharge and SOI also reveal many similarities. The density spectra are very similar to salinity spectra with a few exceptions. Those exceptions are found at depth where the temperature and salinity are related. This allows temperature to influence salinity and hence density. The environmental parameters or physical forcing can be separated according to their dominant periods of variation: either El-Niño – Southern Oscillation (ENSO) periods of less than 10 years or interdecadal periods. The hydrographic parameters primarily have ENSO periods, though the deep waters also have significant interdecadal variations. PDO has both ENSO and interdecadal periods. The upwelling index has approximately equal contributions from ENSO and interdecadal variability and freshwater discharge variations have primarily ENSO periods.

© Copyright by
Nandita Sarkar
2001
All Rights Reserved

To my parents. Jyoti and Biswajit Sarkar.
with love

Acknowledgements

I would like to take this opportunity to thank all those without whose support this endeavour would not have been possible. First and foremost, I would like to thank my advisor, Dr. Tom Royer, for his guidance, help and endless patience. I would also like to thank my committee members, Drs. Chet Grosch, Larry Atkinson and Howard Freeland for their guidance and for reading this manuscript over many, many times. I would like to give a special thanks to Dr. John Klinck for helping me during my early days at CCPO. Thanks are also due to my friend and office-mate, Isaac Schroeder, for his moral support and help, especially during the long nights before the oral defence. Many thanks to my friends and colleagues, Andres Sepulveda, Rosario Sanay, Sinan Husrevoglu, Baris Salihoglu and Hae-Cheol Kim for their comradeship and help. Lastly, I would like to thank my family for their love and support through the good and bad times. Without their faith, I would not have been here.

Table of Contents

List of Tables	ix
List of Figures	xi
1 Introduction	1
2 Background	5
2.1 Environmental Parameters:	8
2.1.1 El-Niño – Southern Oscillation:	8
2.1.2 Pacific (inter)Decadal Oscillation:	9
2.1.3 Freshwater discharge:	9
2.1.4 Upwelling index:	10
3 Methods	11
3.1 Data sets	11
3.2 Influence of temperature and salinity on density	12
3.3 Calculation of mixed layer depths (MLDs)	13
3.4 Maximum entropy method of spectral analysis	14
3.5 Lomb's method of spectral analysis	16
3.6 Preparing data for spectral analyses:	17
3.6.1 Hydrographic data:	17
3.6.2 Environmental parameters:	18
3.7 Analyzing variance of MEM spectral analysis :	18
3.8 Cross-spectral analysis:	19
4 Results and Discussion	21
4.1 Mixed layer depths:	21
4.2 Density profiles	25
4.3 Analysis of spectra:	27

TABLE OF CONTENTS

viii

4.3.1	Hydrographic data:	27
4.3.2	Environmental parameters:	29
4.4	Analysis of variance of peaks	29
4.4.1	Hydrographic data:	30
4.4.2	Environmental parameters:	31
4.5	Cross-spectral analysis	31
4.5.1	Analysis of hydrographic data with depth	31
4.5.2	Analysis of hydrographic data anomalies versus environmental parameters	32
4.5.3	Analysis of temperature and salinity signals	33
5	Conclusions	47
	References	51
	Vita	56

List of Tables

I	Mean annual values of R at different depths at GAK 1	22
II	Trend analysis for MLDs at GAK 1 from 1974 - 1998	25
III	Trend analysis for selected environmental parameters from 1974 - 1998	25
IV	Explained variance for the environmental parameters	31

List of Figures

1	Location of GAK 1 and OSP	6
2	Mixed layer depths (m) from 1974 to 1998 at station GAK 1 . . .	23
3	Selected long-term environmental parameters in the North Pacific from 1974 to 1998. (a) Upwelling Index (m^3s^{-1} per 100 m of coast-line) : (b) Freshwater Discharge (m^3s^{-1}); (c) PDO; and (d) SOI. .	24
4	Two density profiles: one of March 1985 showing good agreement between the 3 methodologies and one of April 1998 (more typical of the area) showing great disparity.	26
5	Average monthly mixed layer depths at GAK 1 along with their standard deviation.	34
6	Spectral analyses of hydrographic parameters at 0 m depth. For all of figures 6 through 14, the 90%, 95% and 99% confidence intervals have been marked on the MEM spectra while the Lomb spectra show 95% and 99% confidence intervals. The periods of the peaks has been indicated in years.	35
7	Spectral analyses of hydrographic parameters at 10 m depth. . .	36
8	Spectral analyses of hydrographic parameters at 20 m depth. . .	37
9	Spectral analyses of hydrographic parameters at 50 m depth. . .	38
10	Spectral analyses of hydrographic parameters at 75 m depth. . .	39
11	Spectral analyses of hydrographic parameters at 100 m depth. . .	40
12	Spectral analyses of hydrographic parameters at 125 m depth. . .	41
13	Spectral analyses of hydrographic parameters at 150 m depth. . .	42
14	Spectral analyses of hydrographic parameters at 175 m depth. . .	43
15	Spectral analysis of selected environmental parameters between 1974 and 1998. The 95% and 99% confidence intervals have been marked on the MEM and the Lomb spectra. The periods of the peaks has been indicated in years.	44
16	Explained variances of (a) ENSO (2-7 years) and (b) Decadal (10-18 years) periodicities in temperature (solid line), salinity (dotted line) and density (dashed line)	45

- 17 Cross-spectral analysis of temperature and salinity at 10 m, 100 m and 175 m. The spectra are normalized and the frequency is in units of *cycles/month*. The phase has been normalized by π 46

Chapter 1

Introduction

The northern Gulf of Alaska is, both ecologically and commercially, a very valuable marine system. This ocean has provided much bounty to generations of native populations who have lived off these seas. Changes in the natural system and changing usage of marine resources will have great implications for the future. To predict future trends, we need a better understanding of the natural variability of the marine system and the closely coupled atmosphere.

One of the mechanisms by which the atmosphere and the ocean interact is through changes in the depth of the mixed layer (MLD) [*Polovina et al.*, 1994; *Mann*, 1993]. The major forcing mechanism of the MLD in this region, wind, is controlled by the position of the storm track. The deepest winter mixed layer is achieved by a small number of winter storms created by the intensification of the Aleutian Low. *Polovina et al.* [1995] suggest that MLDs in the Gulf of Alaska shoaled between 1977-88 compared to 1960-76. This is supported by the study by *Freeland et al.* [1997] who calculate MLDs based on density data from Ocean Station Papa (OSP) (50°N, 145°W). Their study indicates decreasing surface density and a shoaling trend in the deepest winter mixed layer depths. They conclude that primary production in the region will be adversely affected by shoaling because there will be a reduction in the nutrients entrained into the upper ocean every

The journal model for this thesis is the *Journal of Geophysical Research (Oceans)*.

year. However, additional influences on primary production should also be considered. In high latitudes, where light levels change seasonally and light angles are more oblique than at lower latitudes, deepening of the mixed layer can decrease production since it mixes water and organisms into darker zones. In lower latitudes primary production can increase with deepening MLDs as deeper nutrients become additionally available in the euphotic zone. It has been suggested that there is an optimal stability window [Gargett, 1997; Gargett *et al.*, 2001] of the MLD within which primary production is maximized. According to this theory, as water column stability increases and MLDs shoal, northern (Alaskan) stocks will move towards optimal conditions and southern (northern California) stocks will move away from it. The opposite will be the case when water column stability decreases and MLDs deepen.

This theory agrees with observations by Hare *et al.* [1999] that Alaska and (lower) West-coast Pacific salmon stocks are out of phase with one another. In the last few decades, while West-coast salmon production falters, Alaska salmon production flourishes. Although previously it was believed that salmon production is affected by environmental conditions at each stage of its life cycle [Lawson, 1993], recent studies show that salmon production is affected more in the coastal phases of the salmon life cycle rather than the freshwater or deep sea phases [Gargett, 1997]. Considering that sources of food are necessary for the survival of juvenile fish, high primary production would be beneficial to salmon production. Assuming that this significant link between atmospheric conditions and the biology of salmon production is through changing MLDs, the next logical step is to compute the trend of MLDs at the only other station in the Gulf of Alaska other than Line P (including OSP) where hydrographic data are available – GAK 1.

A number of other authors have discussed the role that changing the deepest, winter mixed layer depths played in connecting the atmosphere to the ocean's biology. Namias [1969] discussed the important role played by the Aleutian Low Pressure system in the oceanography of the region. The strength of this system has been found to affect changes in North Pacific fisheries [Brodeur and Ware, 1992; McFurlane and Beamish, 1992; Beamish and Bouillon, 1993; Polovina *et al.*, 1994].

Polovina et al. [1995] calculated mixed layer depths in the Central and North Pacific based on water column temperature observations from 1960 to 1988. They found that the mixed layers in the Gulf of Alaska were 20-30 percent shallower in 1977-88 than during 1960-76. They attributed this change to the intensification of the Aleutian Low and found strong direct correlations between the strength of the Aleutian Low (as given by the Aleutian Low Pressure Index) and salmon and zooplankton production.

Some doubts have been expressed as to the validity of the computations of MLD based only on temperature [*Polovina et al.*, 1995] instead of density that is a function of both temperature and salinity. Time series of salinity measurements are important but rare. The equation of state of seawater [*UNESCO*, 1981], is non-linear so with low temperatures and large salinity ranges, salinity plays a greater role in determining density than temperature. *Freeland et al.* [1997] found that shoaling MLD (based on temperature and salinity) trends at OSP were significant at the 95% confidence level. Although the top of the deeper pycnocline was selected instead of the core, their maximum MLDs corresponded well with the pycnocline. They observed a steady shoaling of MLDs over almost four decades (1956 - 1994). From this they computed a linear shoaling trend of 63 m/century, with a 95% confidence interval of ± 28 m/century. The study also predicted that as the MLDs were shoaling, there should be a declining trend in upper mixed layer nitrate concentrations. The nutrient reduction is caused by a reduced winter entrainment of deep waters with high nutrient concentrations. Since the nutrients in this shallower upper layer could be depleted, this would have an adverse effect on biological productivity. Such a reduction would eventually affect the biological production and the fisheries in the entire N. E. Pacific.

This study focuses on the hydrography at GAK 1 and tries to explain the patterns observed on the basis of some identified 'forcing functions'. The research questions to be addressed are:

1. What are the dynamics that determine the maximum winter MLDs at GAK 1?
2. Which are the important environmental parameters in the region?

3. What are the relative influences of these environmental parameters on hydrographic parameters at GAK 1?
4. Is the N. E. Pacific responding uniformly to these forcing functions?
5. What are the seasonal and interannual effects of temperature and salinity on density at different depths?

The following section gives the background information about the study area and the atmospheric and oceanic processes important here. Based on this, relevant environmental parameters are identified that might be used to explain the observed hydrography. Section 3 describes the data sets used in this study and details quality controls used on them along with a description of the analysis techniques used in this study. These techniques include algorithms used to calculate mixed layer depths and methods to conduct spectral analyses to examine data in the frequency domain. Section 4 presents the results of the analyses and discussions. Section 5 presents the conclusions of this study.

Chapter 2

Background

Gulf of Alaska Station 1 (GAK 1) is the most inshore of a series of hydrographic stations extending south from Seward, Alaska. Situated at $59^{\circ}50.7'N$, $149^{\circ}28.0'W$, it is located at the mouth of Resurrection Bay. The bottom depth is 263 m. The station is in a region where there are a number of glaciers discharging cold freshwater at the surface.

There is a strong seasonality in the wind patterns over the Gulf of Alaska [Wilson and Overland, 1986]. In the summer, the North Pacific High lies over the northern Pacific and the summers are mild. The winds in the region at this time are weak and variable. As winter approaches, the high pressure system retreats southward and it is replaced by the intense Aleutian Low. The weather system of the Gulf of Alaska is dominated by this low pressure system. Thus this region is a major storm dissipation area [Royer, 1998]. The shift in the pressure system between the Pacific High and the Aleutian Low over the Gulf of Alaska gives a strong annual component to the wind stress.

Southcoast Alaska is backed by the Coast Range of mountains with elevations in excess of 4000 m [Royer, 1982]. This has a number of implications. First, these mountains form an orographic barrier to onshore winds. Adiabatic cooling of the air-masses as they are lifted over the orographic barrier causes high rates of precipitation. Second, the mountains create a narrow coastal area as

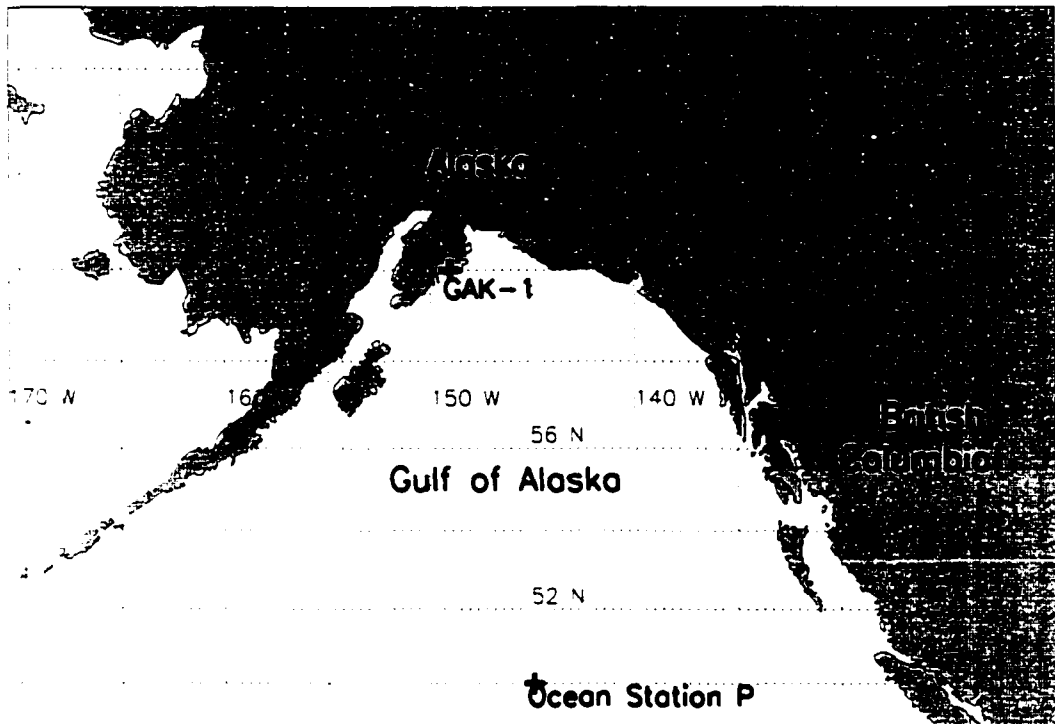


Figure 1: Location of GAK 1 and OSP

drainage basin for the ensuing precipitation. Third, the combination of high latitude and high altitude lowers the snowline sufficiently to permit snowfields to develop [Meier, 1984]. A large number of small streams discharge into the northern Gulf of Alaska. They form a line source of freshwater along the rim of the northern Gulf of Alaska, from British Columbia to about 150°W longitude. This creates an onshore-offshore salinity gradient that drives an alongshore baroclinic jet — the Alaska Coastal Current.

An important aspect of the oceanography of the region is the annual change in Ekman transport due to the shift in atmospheric pressure between the winter low and summer high [Royer, 1975]. Xiong and Royer [1984] describe the hydrology

structure at GAK 1 from 1970-1983. According to their study, annual differences are highly evident at this station. Both the thermocline and the halocline exist simultaneously in the summer. However, they have different mechanisms of formation and/or decay as they are found at different depths. In winter, there is a temperature inversion between 15-200 m and the temperature inversion in spring is at 75 m. The annual temperature minimum occurs in spring for the entire column. The greatest upper layer (< 50 m) salinity was observed in spring while at greater depth (> 150 m) the maximum salinity is observed in late summer. Minimum surface salinity coincides with the temperature maximum in the summer.

The sea surface is in continuous interaction with the atmosphere above it. Some of the interactions are obvious, others are subtle and take place over long time periods. Absorption of short-wave solar radiation increases the temperature of the water. The increase is greatest in surface waters and diminishes rapidly with depth. In the ocean, due to convection or stirring by wind waves, the decrease of temperature with depth does not have a uniform pattern. This stirred layer, having uniform water properties down to some depth from the surface, is known as the surface mixed layer. For the mixing to take place, colder and/or saltier water, that is, denser water, must be displaced upwards against gravity and warmer and/or fresher (lighter) water displaced downwards against buoyancy. The energy required to accomplish this is reflected as a change in the potential energy of the water column [Mann and Lazier, 1996]. Thus mixed layer formation is important from the point of view of energetics or dynamics of the water column. The strength of the pycnocline, i.e. the density difference across the pycnocline at the base of the surface mixed layer, determines the ease with which particles can move across the pycnocline. The pycnocline acts as a barrier to turbulent diffusion of nutrients from deep, nutrient rich areas to the surface euphotic zone and has implications for the 'f' ratio [Eppley and Peterson, 1979]. The 'f' ratio is the ratio of new production to total production. Thus it gives a measure of the portion of total production due to allochthonous nutrient inputs to the euphotic zone.

The surface mixed layer is a product of wind-forcing and other forcing such as

mixing and thermohaline convection, yet it is logical to assume that the greater the wind velocities and the longer their duration, the deeper the mixed layer. After a deep mixing event, when the wind slackens, traces of the deep mixed layer remain until another mixing event is superimposed on it or it is advected out of the region. Since in the Gulf of Alaska, wind stress follows an annual pattern with maximum wind stress and diminished vertical density stratification in winter, the deepest mixed layer should be a “relic” mixed layer [*Sprintall and Roemmich*, 1999] for the year. In this study, this is referred to as a “regional” mixed layer. The “local” mixed layer depth refers to the mixed layer achieved by any mixing event, not necessarily the deepest one.

2.1 Environmental Parameters:

2.1.1 El-Niño – Southern Oscillation:

El-Niño – Southern Oscillation (ENSO) is one of the largest interannual climate signals and it depends on the coupled interactions of the dynamics of the ocean-atmosphere system [*Neelin et al.*, 1998]. According to *Bjerknes* [1969], the ENSO is self-modulating, with SST anomalies in the Pacific driving the varying strength of the trade winds. According to modern understanding of the system, the memory required to switch the phase of the oscillation is provided by the slower timescale of the ocean [*Neelin et al.*, 1998]. *Latif and Graham* [1992] found that significant variability is associated with the subsurface thermal structure. ENSO has periodicities ranging from 2 to 7 years [*Rasmusson et al.*, 1990]. There are two distinct periodicities in this range - a low-frequency, quasi-quadrennial peak of 3-5 years and a weaker peak of around 2 years, called the quasi-biennial peak. ENSO periodicities have been found in many natural signals in almost all parts of the world. This raises questions about the modes of propagation of ENSO. In this study, ENSO is hypothesized to reach the Gulf of Alaska as a Kelvin wave propagating along the coast. This is consistent with studies and observations that ENSO propagates along eastern boundaries of ocean basins as a coastal Kelvin

wave, with associated phase speeds [Meyers *et al.*, 1998]. The Southern Oscillation Index (SOI) [Bjerknes, 1969] has been used here as a measure of ENSO. SOI is based on the pressure difference between Tahiti and Darwin, Australia.

2.1.2 Pacific (inter)Decadal Oscillation:

Decadal and interdecadal signals have been observed repeatedly in the hydrological cycle [Navarra, 1999]. In the late 1970s, there was a significant change in the weather systems in the Pacific climate basin [Namias, 1978]. Mantua *et al.* [1997] proposed a climatic pattern called the Pacific (inter)Decadal Oscillation (PDO) to explain the interdecadal climate variability in the Pacific and define the change in climate in the 1970s as a 'regime shift'. The PDO is defined as the first EOF amplitude of monthly SST anomalies in the Pacific Ocean north of 20°N [Zhang *et al.*, 1997; Mantua *et al.*, 1997]. PDO is not really a forcing function but a spatial pattern of SST. The SOI and PDO are correlated such that cold/warm phase of ENSO coincides with positive/negative polarity of PDO spatially [Mantua *et al.*, 1997].

Although the ENSO and PDO signals are spatially similar, they have considerably different temporal signals. While ENSO consists of quasi-quadrennial and quasi-biennial peaks, PDO has peaks at decadal, bidecadal and pentadecadal periods.

2.1.3 Freshwater discharge:

High rates of coastal freshwater discharge in the northern Gulf of Alaska drives the circulation of the region [Schumaker and Reed, 1980] as a baroclinic jet, the Alaska Coastal Current [Royer, 1982]. However, because there are numerous streams that discharge into the Gulf of Alaska, each of which have their waters locked as snow/ice for part of the year, it is difficult to quantify the amount of freshwater that discharges into the northern Gulf of Alaska. Some attempts have been made to calculate the runoff from water-balance studies and conservation of salt. Assuming vertical flux of salt due to upwelling, Reed and Elliott [1979]

balanced the salt with a combination of discharge and the excess of precipitation over evaporation ($P - E$). Royer [1979, 1981, 1982] has obtained coastal freshwater discharge estimates for the northern Gulf of Alaska (Southeast and Southcoast Alaska). A 150 by 600 km drainage area represents the coastal region. Monthly mean U.S. Weather Service precipitation rates are the input to the model. This precipitation is either allowed to be stored as snow or allowed to be runoff, depending on the monthly mean air temperature. When air temperature rises above freezing, the snow is released slowly over several months from delineated drainage basins.

2.1.4 Upwelling index:

Few wind data are available for coastal locations in this region, especially the open, exposed coasts. Those data that are available are collected too far from the coast to be used in hydrographic analysis. Thus the upwelling index [Bakun, 1973] at 60°N , 149°W is used as a proxy for wind stress. The upwelling index is a measure of the onshore-offshore component of the Ekman transport. The Ekman transport is computed from estimated mean monthly geostrophic wind stress on the sea surface at points near the coast. The Ekman transport is then resolved to calculate the offshore component, the magnitude of which is taken to be an indication of the amount of water upwelled through the base of the Ekman layer to replace water driven offshore by wind stress. The region has, for the most part, a downwelling regime. The upwelling index is negative for most of the year, except briefly in the summer months when the winds are upwelling inducing. The upwelling index has been computed from mean pressure field data computed by the Fleet Numerical Weather Central (FNWC).

Chapter 3

Methods

3.1 Data sets

Hydrographic data versus depth have been collected at GAK 1 since December, 1970 on a quasi-monthly basis. Originally, these were bottle samples at ten discrete depths. STD (Salinity - Temperature - Depth) sampling started in 1974, followed later by CTD (Conductivity - Temperature - Depth) measurements when these instruments replaced the STDs in the late 1970s. Since it was desired to investigate the changes in the mixed layer depth with a finer resolution than the discrete sampling afforded by the bottle data, only STD/CTD data beginning in 1974, with a 1 m depth-sampling interval have been used in this study. Until September 1990, the sampling was quasi-random, based on research vessel ship-of-opportunity sampling, so there are some long gaps in the data set. Since 1990, the sampling is approximately monthly (9 times a year). The original data set has been edited using some quality control measures. First, the casts with depth greater than 275 m were considered not “on station” and thus eliminated as the actual bottom depth is 263 m. For some analyses incomplete casts were also eliminated but the depth up to which the cast was retained varied for different analyses. Second, the casts with temperature, salinity or density anomalies greatly variant from the “normal” were also eliminated. These abnormalities consisted of

spikes which appeared to be due to some sampling error or instrumentation problems. The quality control measures employed were much stricter for those profiles used for the spectral analyses than for the calculation of the mixed layer depths. Some casts accepted for mixed layer depth calculations were shallow casts, but the mixed layer was clearly apparent within the short cast. For the spectral analysis, spectra were calculated for the hydrographic data down to 175 m depth, so deep casts were required for the analysis.

One goal of the present study is to identify the environmental parameters of importance to the hydrography of the region. Four such potential forcing patterns or mechanisms were identified: the Pacific Decadal Oscillation, ENSO, freshwater discharge and upwelling index. They are not necessarily independent of each other but are distinct and significant in their effects on the hydrography of the region. PDO is not, strictly speaking, a forcing function but rather is a spatial pattern of SST. It is thus the result of, and proxy for, thermal forcing. Since the ENSO signal reaches the coast of Alaska as a Kelvin wave, the geostrophic component of the Kelvin wave displaces sub-surface isotherms perpendicular to the direction of wave propagation.

The data for the Pacific (inter)Decadal Oscillation (PDO) are maintained at the URL: <http://tao.atmos.washington.edu/pdo/>

The mean monthly upwelling index data are obtained from: <http://www.pfeg.noaa.gov/>

The SOI data are available at: <http://www.pmel.noaa.gov/>

The freshwater discharge data are taken from: <http://www.ims.uaf.edu/gak1/>

3.2 Influence of temperature and salinity on density

Both temperature and salinity influence seawater density. At low temperatures and small temperature ranges, it is expected that salinity will have a greater

impact on density than temperature. One way to determine this influence [Freeland and Whitney, 2000] is by expressing the stability of the water column as the density gradient:

$$\frac{d\sigma_t}{dz} = \frac{\partial\sigma_t}{\partial T} \frac{\partial T}{\partial z} + \frac{\partial\sigma_t}{\partial S} \frac{\partial S}{\partial z}$$

where σ_t is the water density, z is the depth, T is the temperature and S is the salinity. The two terms on the right hand side give the temperature and salinity influences on density, respectively. A ratio 'R' of these two terms then gives the relative contributions of salinity and temperature on density.

$$R = \frac{\partial\sigma_t}{\partial T} \frac{\partial T}{\partial z} / \frac{\partial\sigma_t}{\partial S} \frac{\partial S}{\partial z}$$

At each depth, four values of sigma-t are computed using the range of temperature and salinity values. Since the Equation of State [UNESCO, 1981] is non-linear, the temperature influence is determined by calculating the range of sigma-t using the range of temperature (maximum - minimum) with a mean salinity [Fofonoff, 1985]. The salinity influence is calculated in a similar manner by determining the range of sigma-t from the mean temperature and range of salinity. These calculations were done for each depth and each month of the year. For the depth range in this study, the effect of pressure is taken to be negligible. An R of unity indicates equal influence of salinity and temperature on density, a value greater than unity indicates greater influence of temperature and a value less than unity indicates greater influence of salinity.

3.3 Calculation of mixed layer depths (MLDs)

Another goal of this study is to compare the MLDs obtained for GAK 1 to those obtained by Freeland *et al.* [1997] for the central Gulf of Alaska in order to determine whether similar conditions occur in the northern Gulf of Alaska. Three independent methodologies have been used to calculate the deepest winter MLDs. The first is an algorithm based on the method used by Freeland *et al.* [1997]. This involves the fitting of a step function to the upper ocean density distribution. The best fit of a two-layer structure is determined using a least-squares technique

where the depth of the upper mixed layer, h , is found. While *Freeland et al.* [1997] have used 300 m as the maximum depth of the two-layer system H , in this study it has been changed due to shallower depth of the station. The maximum depth of 263 m is used for H . This would be an acceptable choice as *Freeland et al.* [1997] have found that the method is not sensitive to a choice of H between 200 and 500 m. Once h is determined, the depth of the lower layer is known ($H - h$) and the mean densities of the upper and lower layers can be determined.

The other two independent methodologies are visual examinations of the density profiles. Two investigators (N. Sarkar and T. Royer) separately examined the density profiles to determine the most appropriate depth of the deepest winter mixed layer. These have been used as a check for the method computing MLDs from the algorithm. A statistical test is made to check whether the three sets of MLDs are correlated. The significance of the trend found in the MLD time series is then tested using Mann statistics. The Mann statistics tests whether there is a statistically significant trend in a time series. It is a non-parametric test based on Kendall's tau and is thus a more robust test than parametric ones [*Kendall and Gibbons*, 1990]. Trend analysis is carried out on potential environmental parameters like freshwater discharge, upwelling index and PDO over the same period of time.

3.4 Maximum entropy method of spectral analysis

The maximum entropy method (MEM), using the Burg algorithm [*Ulrych*, 1972], is a popular method of spectral analysis because of its property of high resolution at low frequencies. The MEM spectrum of a stationary, random, uniformly sampled process is the spectrum that results from maximizing the entropy of that process. Information is defined as: $I_i = K \log(1/p_i)$ where K is a constant and p_i are the probabilities of occurrence. The average information per time interval (T), represented by \mathcal{H} , is called entropy and defined [*Shannon*, 1948] as:

$$\mathcal{H} = \frac{I_{total}}{T} = -K \sum_{i=1}^M p_i \log p_i$$

Entropy is thus the measure of disorder in a system. The probability distribution that maximizes the entropy is numerically identical with the frequency distribution which can be realized in the greatest number of ways [Jaynes, 1968]. To apply the concept of maximum entropy to spectral analysis, the relation between the entropy rate for an infinite process is related to the spectral density $S(f)$ of a stationary Gaussian process as:

$$\mathcal{H} = \frac{1}{4f_N} \int_{-f_N}^{f_N} \log S(f) df$$

where f_N is the Nyquist frequency. Rewriting in terms of the autocorrelation $\phi(k)$:

$$\mathcal{H} = \frac{1}{4f_N} \int_{-f_N}^{f_N} \log \left[\sum_{k=-\infty}^{\infty} \phi(k) \exp(-i2\pi f k \Delta t) \right] df$$

where Δt is the uniform sampling rate. Maximizing this with respect to the unknown $\phi(k)$ under the condition that $S(f)$ must also be consistent with the known autocorrelations $\phi(0), \dots, \phi(M-1)$ gives the MEM spectral estimate. This approximation gives the maximum uncertainty with respect to the unknown information while being consistent with the known information [Ulrych and Bishop, 1975]. The number of degrees of freedom is calculated by taking the ratio of the total number of data points to the number of coefficients calculated.

To define confidence limits for the maximum entropy spectra, a red spectrum is used. It is assumed that the red spectrum is that of an AR(1) process and is derived as [Priestly, 1981]:

$$S_R(f) = \frac{1 - \rho_1^2}{1 - 2\rho_1 \cos(2\pi f \Delta t) + \rho_1^2}$$

where ρ_1 is the autocorrelation function at lag 1, f being the frequency. Thus deviations from this spectrum have a chi-squared distribution. The values for the confidence limits are then obtained by looking up the multiplicative factor from the chi-square distribution table, using the degrees of freedom for the required probability.

3.5 Lomb's method of spectral analysis

Spectral analysis is used to partition the variance of a time series as a function of frequency. For a stochastic time series, contributions from the different frequency components are measured in terms of the power (energy per unit time) spectral density [Emery and Thomson, 1998]. The Lomb method [Lomb, 1976] evaluates data (and sines and cosines) only at times t_i that are actually measured. For N data points, if F is any hydrographic variable or forcing function, $F_i \equiv F(t_i)$, $i = 1, 2, \dots, N$, and the mean and variance are calculated as:

$$\bar{F} \equiv \frac{1}{N} \sum_{i=1}^N F_i$$

$$\sigma^2 \equiv \frac{1}{N-1} \sum_{i=1}^N (F_i - \bar{F})^2$$

Then the normalized (by the variance) Lomb periodogram (spectral power as a function of angular frequency, $\omega = 2\pi f > 0$) is defined by:

$$P_N(\omega) = \frac{1}{2\sigma^2} \left\{ \frac{[\sum_j (F_j - \bar{F}) \cos \omega(t_j - \xi)]^2}{\sum_j \cos^2 \omega(t_j - \xi)} + \frac{[\sum_j (F_j - \bar{F}) \sin \omega(t_j - \xi)]^2}{\sum_j \sin^2 \omega(t_j - \xi)} \right\}$$

where ξ is defined by the relation:

$$\xi = \frac{1}{2\omega} \arctan \frac{\sum_j \sin 2\omega t_j}{\sum_j \cos 2\omega t_j}$$

The scaling with ξ has two major effects:

- (i) It makes $P_N(\omega)$ independent of shifting all the t_i 's by any constant.
 - (ii) It weighs the data on 'per point' basis, instead of a 'per time interval' basis.
- The Lomb method can be used for unevenly spaced data whereas fast Fourier transform (FFT) and maximum entropy techniques require uniformly spaced data.

The normalization of the Lomb periodogram facilitates finding significance of the peaks in the spectrum $P_N(\omega)$. The null hypothesis states that the spectrum is 'white', ie. the spectral constituents have near-equal amplitude throughout the frequency range [Emery and Thomson, 1998] i.e. the data values are independent Gaussian random values. Thus in the case of the null hypothesis, at any particular ω , $P_N(\omega)$ has an exponential distribution with unit mean. Thus,

$$P(> \eta) \equiv 1 - (1 - e^{-\eta})^M$$

for M independent frequencies between any given η and $\eta+d\eta$, η being any spectral density level normalized by the variance. P is the probability that a value greater than η would be found by chance. Thus the significance is $1 - P$.

The Lomb method of calculating power spectra, though very powerful, is not suitable for low frequency events like decadal and inter-decadal signals due to the assumption that the data are “white”. It is used here as a check for the MEM spectra for the high frequency portions of the spectra.

Spectral analysis is done on the temperature, salinity and density data at selected depths and also on the forcing patterns and functions. To quantify the effect of the environmental parameters on the hydrography, the anomalies of the time series of the hydrographic data have been cross correlated with the forcing function and pattern anomalies. Annual signals in all data sets have been extracted since these signals would correlate well regardless of any potential relationships.

3.6 Preparing data for spectral analyses:

3.6.1 Hydrographic data:

After quality control measures, there were 205 out of 257 hydrographic profiles remaining over the period from 1974 to mid-1998. These data are not evenly spaced and especially in the 1970s and early 1980s, there are large gaps in the data sets. Lomb’s method can be used with these data, but the maximum entropy method requires equally spaced data. Thus the data were linearly interpolated to fill the gaps and the interpolated data set has 295 monthly observations, from January 1974 to July 1998.

The means were removed from the data and these departures from the mean were used for spectral analysis. Before the spectral analyses, a quadratic was removed to eliminate a possible very low frequency or trend. Initial results from

the spectral analyses showed a very strong annual component to the hydrographic signal. The annual signal was stronger at the surface and weaker at depth. To address the low frequency signals, the annual signal was removed. The monthly means were used as the annual signal as this truly eliminated the total annual frequencies. The number of coefficients in the maximum entropy method is set to 150, while the total number of interpolated data points is 295, so that the effective degrees of freedom is 2.

3.6.2 Environmental parameters:

The environmental parameters (forcing functions and patterns) were analyzed over the same period as the hydrographic data. All the environmental parameters used here had regular monthly data, with no unusual deviations or gaps, so no quality control or interpolation was performed on them. As usual, the departures from the mean were used for spectral analysis. The PDO, discharge and upwelling index had strong annual signals, which were removed along with a quadratic trend. In addition, the discharge data had a large semi-annual signal due to the passage of the Aleutian Low pressure system and the spring melt. Thus, for the discharge data, after removal of the annual and a quadratic, the semi-annual signal and another quadratic were removed. Only a quadratic trend was removed from the SOI data as it did not have concentration of energy in high frequencies. For consistency, the effective degrees of freedom was maintained at 2 for the maximum entropy method.

3.7 Analyzing variance of MEM spectral analysis :

The significant peaks obtained by the maximum entropy method are analyzed for the explained variance. In this analysis, all peaks above the 90% confidence interval have been considered to be significant and were used to calculate their contribution to the variance. Each peak is assumed to be a result of a sinusoidal

signal composed of sine and cosine components. The least-squares method is used to calculate the amplitude and phase of the constituent harmonic which is then fitted and removed from the original signal. The variance is calculated both before and after the removal of the fitted harmonic. The ratio of the variance of this harmonic to the original (initial) variance gives the explained variance for that frequency. In this manner, the frequencies associated with the significant peaks in the signals are systematically removed from the original signals and explained variances are calculated for each peak.

The spectral peaks which have been considered for analysis of variance have been divided into two classes according to their periodicities. The peaks with periodicities between 2 and 7 years have been grouped together as ENSO-like periodicities and the sum of their explained variances has been calculated at each depth. The peaks with periodicities between 10 and 16 years have been classed together as decadal periodicities and the sum of their explained variances have also been calculated at each depth.

For this method, only those casts have been considered which go down to at least 250 m. There are 183 such casts which have been interpolated to 295 monthly values from January 1974 to July 1998. A quadratic trend has been removed from these time series. The MEM (normalized) spectra have been calculated and the explained variance is based on the peaks obtained by this method. Since the spectra are normalized, the explained variances in the different hydrographic signals at the different depths can be directly compared.

3.8 Cross-spectral analysis:

Cross-spectral analysis is done to compare spectra of time series to see if they are coherent and if they have a stable phase relationship. The spectra were first calculated using Fourier methods with the Parzen filter as a spectral smoother. The coherency gives a measure of the energy in the cross-spectrum compared to the energy in the geometric mean of the spectra. The phase lag between the two spectra is then calculated, normalized by π . The coherency and phase are

relevant only in the window when there is substantial energy in both spectra. This requirement sometimes makes it difficult for some spectra to be compared with others.

In the present study, cross-spectral analysis has been used in three distinct ways. Cross-spectral analysis has first been used to confirm that spectral signals in the hydrographic data are consistent throughout the water column. Thus cross-spectral analysis was carried out between the signal at the 10m depth and successively greater depths. The signal at the surface was not considered due to the higher 'noise' level. Second, cross-spectral analysis has been carried out between the environmental parameters and the hydrographic data at selected depths to find the coherence and the phase difference between them. Third, temperature and salinity spectra at selected depths (10 m, 100 m and 175 m) were cross-correlated to estimate their interdependence.

The preparation of the data sets for cross-spectral analysis to determine the consistency of the spectral signals and for the cross-spectral analysis between the environmental parameters and the hydrographic data required removal of the annual means to determine anomalies. The linear and quadratic trends were also removed from each data set to detrend the data. All the spectra have been normalized by their standard deviations to allow comparison among them. For the cross-correlations of the temperature and salinity data, the annual signal was retained for analysis but the mean and the quadratic were removed. The annual signal is used to compare the spectral signal coupling at the annual frequency, where both temperature and salinity have a high amount of energy.

Chapter 4

Results and Discussion

4.1 Mixed layer depths:

The relative influences of temperature and salinity on density at selected depths are given by the ratio 'R' (Table I). The values of R are considerably less than 1 and range from 0.1263 to 0.1529. The annual means vary from 0.1385 at the surface to 0.1521 at the bottom. R is highest in the spring and lowest during summer. The range of R is uniform (~ 0.0025) from 50 m to 250 m. The values increase deeper in the water column, suggesting a lesser influence of salinity on density with depth. However, the values still remain well below unity. So, though the effect of salinity is reduced at depth, it is still significant. The R values show that salinity has a greater influence on density than temperature at GAK 1 throughout the year and over the entire water column. During winter and spring, when freshwater is locked up as snow and ice, the importance of salinity is slightly lower. In summer, snow and ice melts, releasing freshwater and the role played by salinity is even greater. The importance of salinity also decreases deeper in the water column. This is because the influx of freshwater is at the surface and salinity range decreases deeper in the water column.

The three independent MLD calculations at GAK 1 show a deepening trend during 1974-1998 (Fig. 2). The rates for the deepening trends (Table II) range from more than 100 m/century for the data set returned by the two-layer algorithm

TABLE I: Mean annual values of R at different depths at GAK 1

Depth in m	Mean annual R	Maximum R	Minimum R
0	0.1385	0.1464	0.1263
10	0.1420	0.1467	0.1334
20	0.1436	0.1470	0.1368
50	0.1465	0.1475	0.1449
75	0.1477	0.1487	0.1462
100	0.1486	0.1497	0.1475
125	0.1493	0.1505	0.1480
150	0.1500	0.1515	0.1487
175	0.1506	0.1522	0.1494
200	0.1513	0.1525	0.1499
250	0.1521	0.1529	0.1505

and set 1, to about 50 m/century for data set 2. However, no trends are significant as the probability of being able to accept the null hypothesis of no significant trend is very high. The probability is calculated from Kendall's τ and the significance is given by 1 - probability. A value of 90% or more is considered to be significant in this study. It is possible that the lack of significance is due to the short time series, and given a longer record, the deepening trend could become significant. The difference in the trends of MLDs at GAK 1 (non-significant deepening) from the trend at OSP (significant shoaling) is probably a result of the differences in their physical location – GAK 1 is at the edge of the Alaskan gyre, while OSP is located in the center of the gyre. This difference may be due to the different effects of environmental parameters at the center and edge of the gyre. Trends of the environmental parameters (Fig. 3) have also been analyzed (Table III). Whereas there are no significant trends in upwelling index and freshwater discharge, there is a (marginally) significant trend in SOI during 1974-1998. The 'trend' in PDO might be a part of a longer cycle since PDO appears to have a periodicity of 40 - 50 years [Mantua *et al.*, 1997].

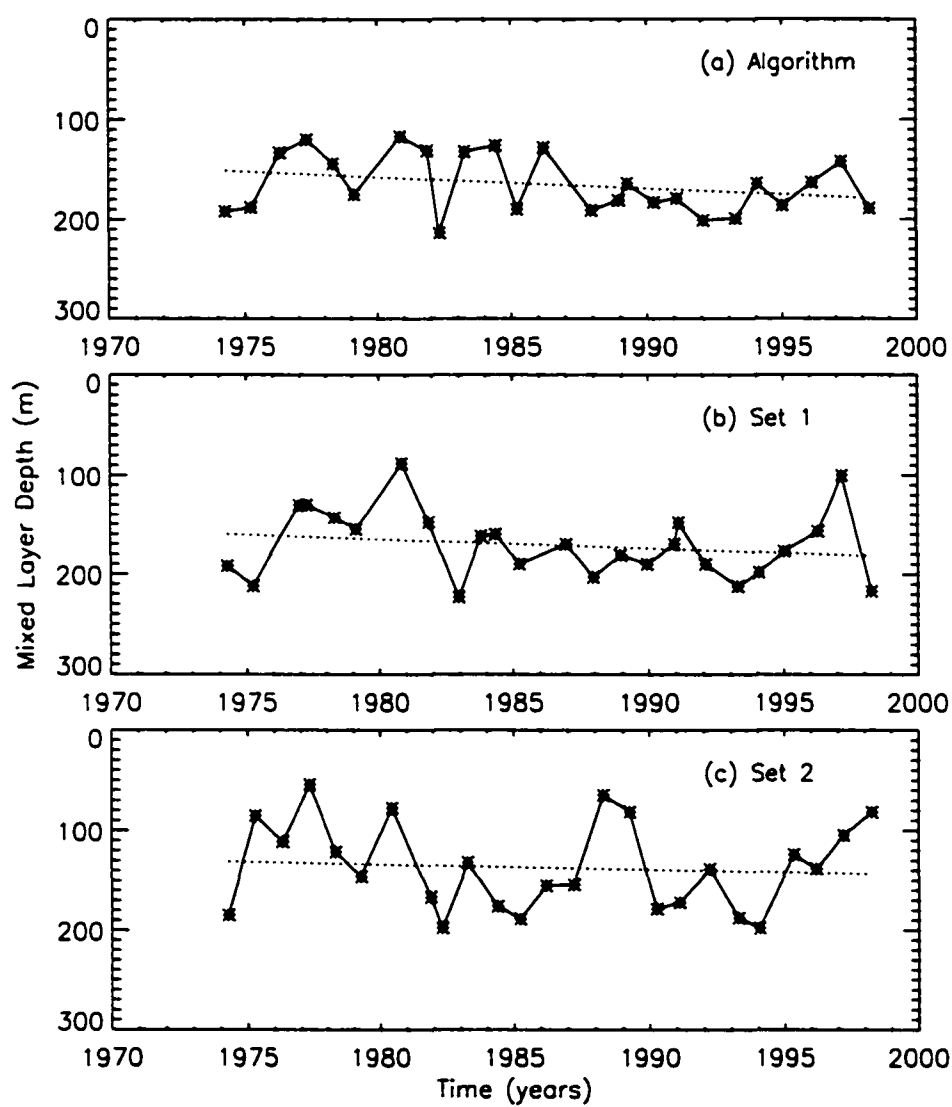


Figure 2: Mixed layer depths (m) from 1974 to 1998 at station GAK 1

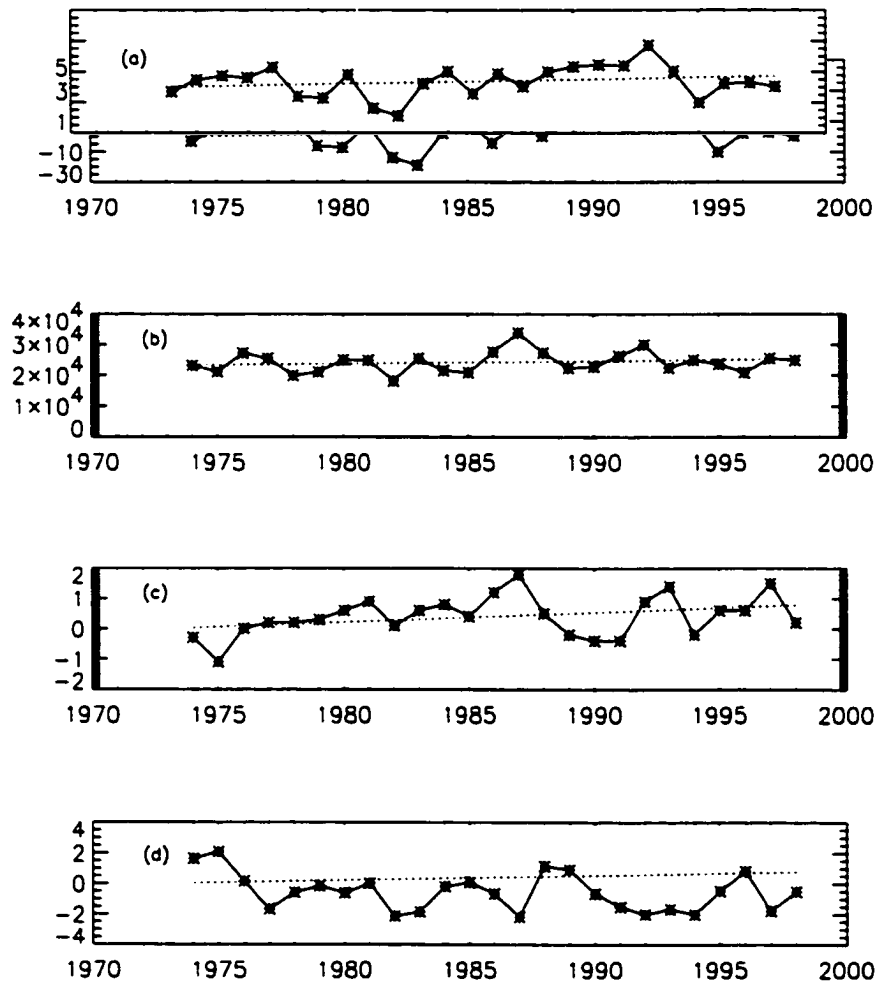


Figure 3: Selected long-term environmental parameters in the North Pacific from 1974 to 1998. (a) Upwelling Index ($m^3 s^{-1}$ per 100 m of coastline); (b) Freshwater Discharge ($m^3 s^{-1}$); (c) PDO; and (d) SOI.

TABLE II: Trend analysis for MLDs at GAK 1 from 1974 - 1998

Null Hypothesis: There is no significant trend in the data set.				
Data Set	Deepening trend (m/century)	Kendall's τ	Probability that null hypothesis is true	Significance
Algorithm	116	0.147	0.302	no
Set 1	114	0.223	0.118	marginal
Set 2	52	0.060	0.673	no

TABLE III: Trend analysis for selected environmental parameters from 1974 - 1998

Null Hypothesis: There is no significant trend in the data set.			
Data Set	Kendall's τ	Probability that null hypothesis is true	Significance
Upwelling Index	0.177	0.215	no
Freshwater Discharge	0.102	0.484	no
PDO	0.259	0.070	yes
SOI	-0.227	0.112	marginal

4.2 Density profiles

The density profiles often contain a number of step-like features reminiscent of earlier mixed layers (Fig. 4). For example, the density profile of March 1985 shows a surface mixed layer between 10 and 20 m depth. The profile slope is then smooth until the depth of 190 m. where there is a sharp gradient that can be considered the deepest winter mixed layer. For this profile, the three methods to calculate MLDs show good agreement. Such profiles are uncommon. More often the profiles look like the one of April 1998 (Fig. 4). This profile contains more than one sharp gradient change at different depths. Two of the methods choose two different breaks in the profile as the mixed layer depth, while the algorithm

chooses a depth between the two. As a result, it is difficult in many cases to actually identify the deepest winter MLD. This suggests the influence of other processes affecting the MLD at GAK 1.

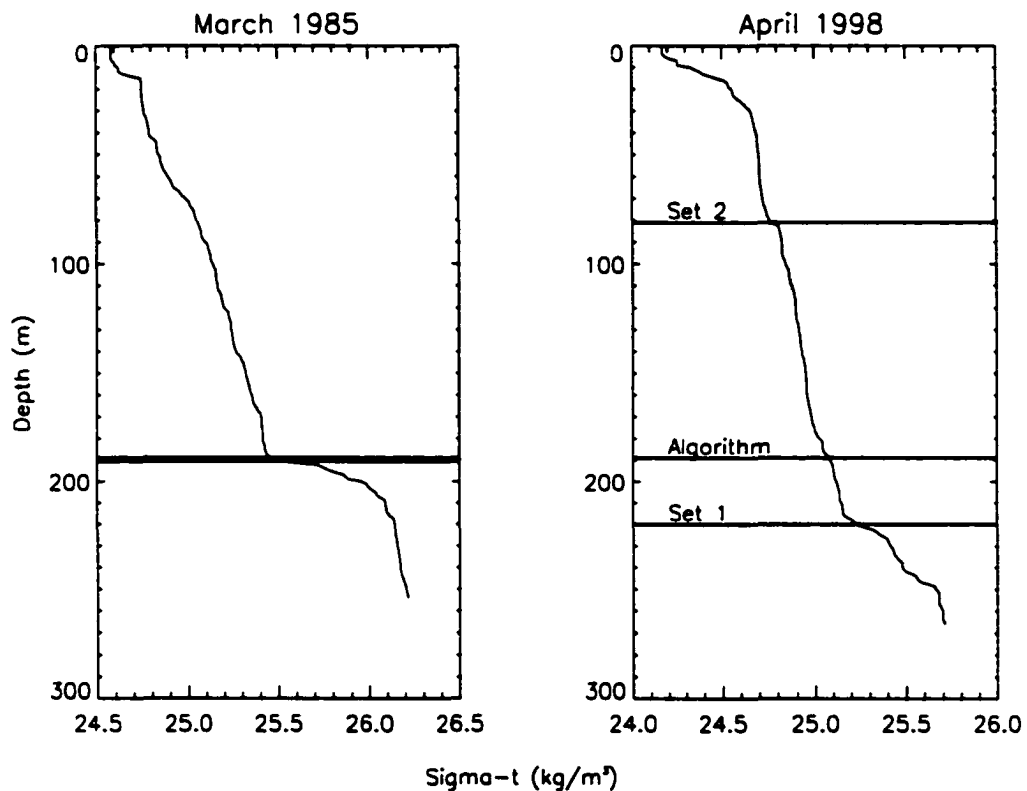


Figure 4: Two density profiles: one of March 1985 showing good agreement between the 3 methodologies and one of April 1998 (more typical of the area) showing great disparity.

To investigate these other potential processes, mean depths of the MLDs were plotted for each month and their standard deviations were overplotted (Fig. 5). The summer months of July to September have small standard deviations. The winter months, on the other hand, have very high standard deviations and this could be a reason why it is difficult to calculate winter MLDs in this region. There can be a number of explanations for this. High standard deviations are due to highly episodic events. GAK 1 is situated at the edge of the gyre, where

both downwelling winds and the Alaska Coastal Current should have significant influences. This will cause high variability in the hydrography at GAK 1. Since the greatest variability is in winter, the cause of these great variations is the wind stress and the maximum density is due to the minima in temperature and freshwater discharge.

4.3 Analysis of spectra:

4.3.1 Hydrographic data:

The MEM temperature spectra (Figs. 6-14) have regular variations with depth. The temperature variability of the surface layer consists of a two-year signal (2.6 years) and a decadal signal (8.5 years) (Fig. 6). Between 10 m and 20 m (Figs. 7 and 8), a decadal signal is seen along with a two-year period. At 50 m (Fig. 9), although the peaks are much closer to the confidence intervals, the dominant period is still at about 2 years. Between 75 and 150 m (Figs. 10 to 13), ENSO periodicities are clearly seen. Unlike at the surface, where most of the energy is in the 2.6 year peak, the energy at these depths is contained primarily in the 3.7 year peak and in the 5.2 year peak. At 175 m, there are ENSO periodicities, along with a bidecadal signal of 16 years (Fig. 14).

The MEM salinity spectra (Figs. 6-14) have less variation with depth than the temperature spectra. At 0 m (Fig. 6) and at 10 m (Fig. 7) there are no peaks above the 99% confidence limit. However, at the surface (0 m) there are peaks in the ENSO band of 4 years and two-year period of 2.1 years which are above the 95% confidence limit. At 10 m, the only peaks above the 95% confidence limit are at the decadal frequency of 11.5 years and at 2.1 years. At 20 m (Fig. 8), there is a decadal peak (11.5 years) which is of significance at the 99% level. At 50 m (Fig. 9) and 75 m (Fig. 10), ENSO periodicity of 3.7 and two-year periodicity of 2.7 years are significant at the 99% level. In addition, at 50 m, the ENSO period of 5.3 years is also significant (99%). Between 100-150 m (Figs. 11-13), all the peaks are lower but broader. None are significant at the 99% confidence level.

More energy is found in longer periods (more than 5 years) at these depths. At 175 m (Fig. 14), there is a significant peak of ENSO frequency (3.1 years).

The MEM density spectra (Figs. 6-14) have the least variation with depth. At the surface (0 m) (Fig. 6), there are no peaks above the 99% confidence limit, but as in the salinity spectrum at this depth, above the 95% confidence limit, there are two peaks at 4 and 2.1 years. At 10 m (Fig. 7), the only peak above the 99% confidence limit is at the period of 2.1 years. At 20 m (Fig. 8), the 2.6 year period becomes significant, along with a decadal period of 11.1 years. At 50 m (Fig. 9), the dominant signal is ENSO, with the 3.7 year periodicity having the highest peak. At 75 m (Fig. 10), ENSO is still dominant, but the two-year peak at the 2.6 year period is smaller, though still above the 99% confidence limit. At 100 m (Fig. 11), ENSO dominates with the highest peak at 3.7 years. From 125 m to 175 m (Figs. 12-14), the dominant signal has a period of 14-16 years and ENSO periodicities can also be seen.

The density spectrum at any particular depth does not look necessarily similar to either the temperature or the salinity spectrum at that depth. At the surface, the density spectrum is almost identical to the salinity spectrum. From 20 m down to 75 m, the salinity and density spectra still look very similar. At 100 m and below, the density spectra look different from the salinity spectra. The temperature spectra at the same depths differ from the density spectra. As one goes down the water column, the influence of salinity diminishes slightly, but is still dominant over temperature. At the surface, the salinity influence is still the highest and the density and salinity spectra look similar. Deeper in the water column, the temperature variations modify the density spectra more, so that the density spectra look more like a composite of the temperature and salinity spectra. It is also interesting to note that of the ENSO periodicities, the 3.7 year period is the dominant one in the water column for all three hydrographic parameters.

The spectra obtained by Lomb's method are slightly different from the MEM spectra. These spectra have been calculated as a check for the MEM spectra. Even though the peaks are lower and broader than the peaks obtained by MEM, the area under the curves is preserved in the two methods and the spectra are fairly

consistent. One peculiarity of the Lomb method is that low frequency signals like 16.6 years appear often in the spectra. This might be an artifact of the method.

4.3.2 Environmental parameters:

In order to examine whether the hydrography has significant energy at frequencies similar to those of the potential forcing functions and patterns, the MEM and Lomb spectra of the environmental parameters were calculated (Fig. 15). The MEM and Lomb spectra of both PDO and upwelling index are similar. Both have energies at decadal low frequencies (13.9 - 15.9 years) and at ENSO frequencies (3 - 6 years). The MEM spectrum for SOI has some distinct, high but broad peaks at typical ENSO frequencies of 5 and 3.6 years and a two-year peak. The highest peak is that of the 5 year period. The MEM spectrum of the upwelling index has a peak at 14.5 years that is above the 99% confidence limit. Peaks at ENSO periodicities are not significant above the 99% level.

The analysis shows that the PDO signal seems to be composed of a bidecadal periodicity and ENSO periodicities. In contrast, the upwelling index can be said to consist of the bidecadal periodicity. The freshwater discharge shows primarily the influence of ENSO periodicities and some influence of the bidecadal periodicity. While the 5 year peak is the most dominant in the SOI, the PDO has a dominant peak of 3.2 years (ENSO period). The freshwater signal seems a composite of the PDO and SOI signals.

4.4 Analysis of variance of peaks

Although spectral analysis gives an indication that the energy is concentrated under the peaks, it is difficult to estimate the variance accounted for by each peak by spectral analysis alone. First, the explained variance is a function of the area under the peak. This includes both the height and the breadth of the peak. A peak that is short but broad can account for as much or more variance than a tall, sharp peak. Second, the spectra calculated here are normalized by their standard

deviation. So they do not give a measure of absolute variance. This necessitates the analysis of variance of the spectral peaks.

4.4.1 Hydrographic data:

Figure 16 shows the depth dependence of the explained variances of the two broad frequency classes - ENSO and decadal. The ENSO signals in this context contain the periodicities between 2 and 8 years while decadal periodicities are those between 10 and 17 years. At almost all depths, ENSO explains more variance than the decadal signal. The two signal classes are comparable in magnitude only in the surface layers, from the surface down to 20 m. Between the depths of 50m and 150m, almost 50% of the energy is in ENSO frequencies. There is almost no energy in the decadal frequencies at these depths, except for a slight amount (10%) in the salinity signal. Below 150 m, the variance explained by the ENSO frequencies is approximately double that explained by the decadal frequencies.

Temperature, salinity and density do not have identical explained variance patterns with depth. For the ENSO frequencies, density and salinity have similar shaped curves, but density contains more ENSO variance than salinity at almost all depths. The exceptions are near the surface and at a depth of 200 m. In addition, the maximum ENSO variance in salinity is shallower (50 m) than in density (75 m). The temperature signal does not have a minimum in variance at ENSO frequencies at 10 m, unlike both salinity and density but has a minimum at 20 m. It also has a sub-surface maximum at 100 m. From this depth down to the bottom (250 m), there is a steady decrease in energy at ENSO frequencies in the temperature spectra. But ENSO is seen more clearly in the temperature signal than in either salinity or density signals between 100 and 250 m.

Energy at decadal frequencies is less than 20% for all the hydrographic parameters, at all depths. There is a sub-surface minimum in energy at decadal frequencies which corresponds closely to the sub-surface maxima in energy at ENSO frequencies. There are no well defined maxima at any depth.

4.4.2 Environmental parameters:

An analysis of variance of peaks in MEM spectra was done for the environmental parameters to compare the energies in certain periodicities (Table IV). Once again two period classifications were made: one at ENSO periods and another at decadal frequencies as explained previously. The SOI 1974-1998 time series contains ENSO periodicities of ~ 2.5 , 3.5 and 5 years. These explain 32% of the total variance. The annual 1974-1998 time series of PDO also contains ENSO periodicities and a bidecadal period and together they explain more than 40% of the total variance. The time series of upwelling index from 1974 to 1998 shows bidecadal oscillation as well as ENSO. However, the energy in these periodicities is much less compared to the energy in the annual signal, which has been removed. Freshwater discharge has 20% of its energy in ENSO and bidecadal periodicities, with ENSO containing the majority of the variance.

TABLE IV: Explained variance for the environmental parameters

Environmental Parameters	% of Variance	
	ENSO	Decadal
SOI	32.48	-
PDO	30.34	10.67
Upwelling Index	3.29	3.22
Freshwater Discharge	18.44	2.08

4.5 Cross-spectral analysis

4.5.1 Analysis of hydrographic data with depth

Although two or more spectra may have energy in the same periodicities, these signals may or may not be coherent. The coherence is tested by cross-spectral analysis. This analysis produced voluminous data, which are not shown here. A brief description of the results is given instead. The spectra of the hydrographic

parameters at each of the pre-selected depths have energy primarily concentrated at periods greater than 4 years. At such low frequencies, the phase shift is too small to be measurable. The coherence between the temperature spectrum at 10 m and other spectra is almost 1 near the surface, but as one goes deeper in the water column, the coherence decreases from 1 to 0.8. The salinity and density spectra, however, show less coherence and more phase difference with depth.

4.5.2 Analysis of hydrographic data anomalies versus environmental parameters

This analysis also yielded a large amount of data which is summarized here. As expected, PDO is highly correlated with near-surface (10m) temperature anomaly, with temperature anomaly lagging PDO by an order of a few months. Both near-surface salinity and density anomalies have very low coherence and higher phase differences with PDO in the low-frequency region. Conversely, salinity and density anomalies at 10 m are much more coherent than temperature anomaly to freshwater discharge. Salinity and density are also in phase with freshwater, while temperature shows a small phase lag. However, these phase relationships are at very low frequencies (17 years) and must be studied carefully as FFT does not perform well at such low frequencies. The comparison of the temperature anomaly spectrum at 10 m with the spectrum of freshwater discharge anomaly is a little difficult due to non-comparable energies in their spectra. SOI also has a high coherence and a small phase difference with temperature anomaly at 10 m. Salinity and density anomalies have low coherence and higher phase difference with SOI at a depth of 10m. Upwelling index anomaly has a small phase difference with each of temperature, salinity and density anomalies (hydrography lags upwelling index) and a high coherence of 0.8.

Although this analysis is not sufficient to determine a cause-effect relationship, it does show a higher coupling of temperature with PDO and SOI and a higher coupling of salinity and density with freshwater discharge. This analysis also shows that while temperature behaves in a markedly different manner, salinity

and density have similar behavior with respect to these environmental parameters.

4.5.3 Analysis of temperature and salinity signals

The temperature and salinity signals have been cross-correlated at the selected depths of 10 m, 100 m and 175 m (Fig 17). At 10 m, almost all the energy of both signals is in the annual signal. The coherence is very high here and the salinity signal lags the temperature signal by about 2-3 months. A high air temperature causes snow/ice to melt and enter the area as freshwater discharge, that then lowers the salinity at 10 m. at a later time in the year. Also, the autumn storms follow the relatively quiescent summer period when SST reaches its maximum. At a depth of 100m, the energy in the annual frequency in both signals is slightly diminished. There is considerable energy centered at a frequency of about 4 years (ENSO frequencies). The spectra under both these peaks are highly correlated with a slight phase difference, of the order of a few months. At 175 m, the temperature spectrum has energy at both the annual and ENSO frequencies, while salinity has all its energy in the annual signal. Thus only the annual frequency can be compared. At this frequency, the coherence continues to be high and the phase difference is reduced to about a month.

The high coherence of the spectra, mostly at annual frequencies, shows that temperature and salinity are not completely independent variables. They are highly correlated and are influenced by similar or related forcing functions. Because of this, although salinity has a greater influence on the density of the region than temperature, the density spectrum is not always similar to the salinity spectrum. The freshwater discharge is from the surface and the highest range of salinity is at or near the surface. The values of 'R' are lowest here, and thus, near the surface, the density spectra look most like the salinity spectra. At the surface they are almost identical. Deeper in the water column, the value of 'R' increases as the range of salinity decreases. Since the temperature and salinity are highly correlated, the density spectra then take on attributes from both of them.

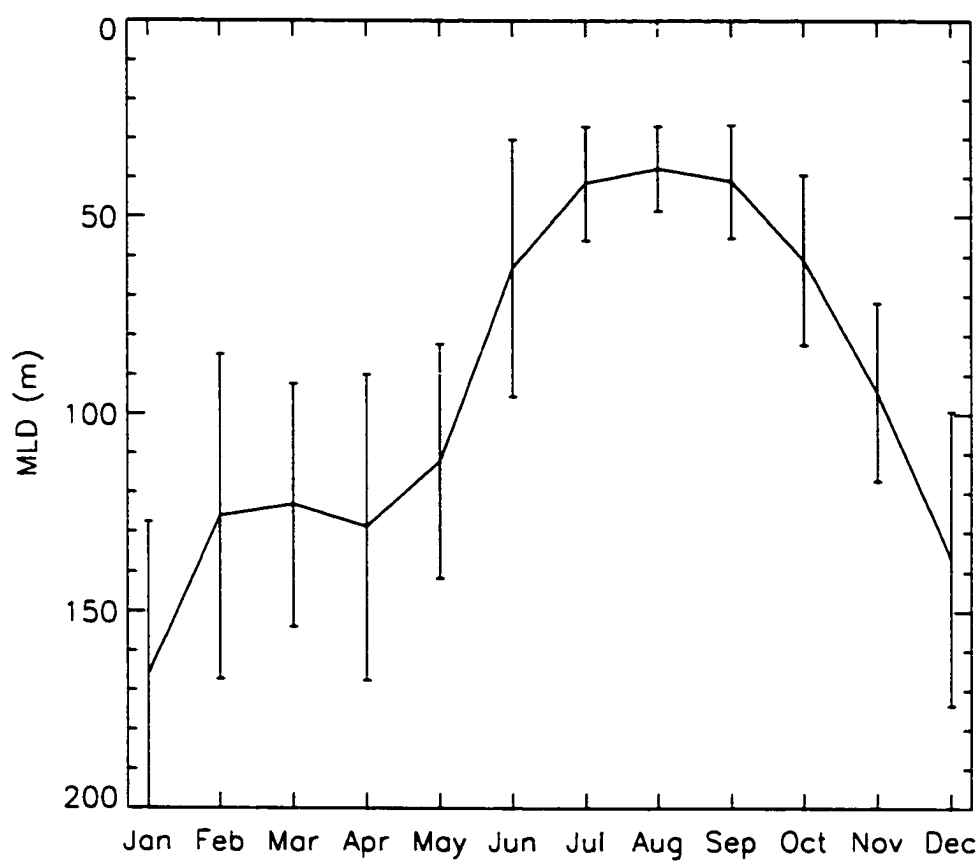


Figure 5: Average monthly mixed layer depths at GAK 1 along with their standard deviation.

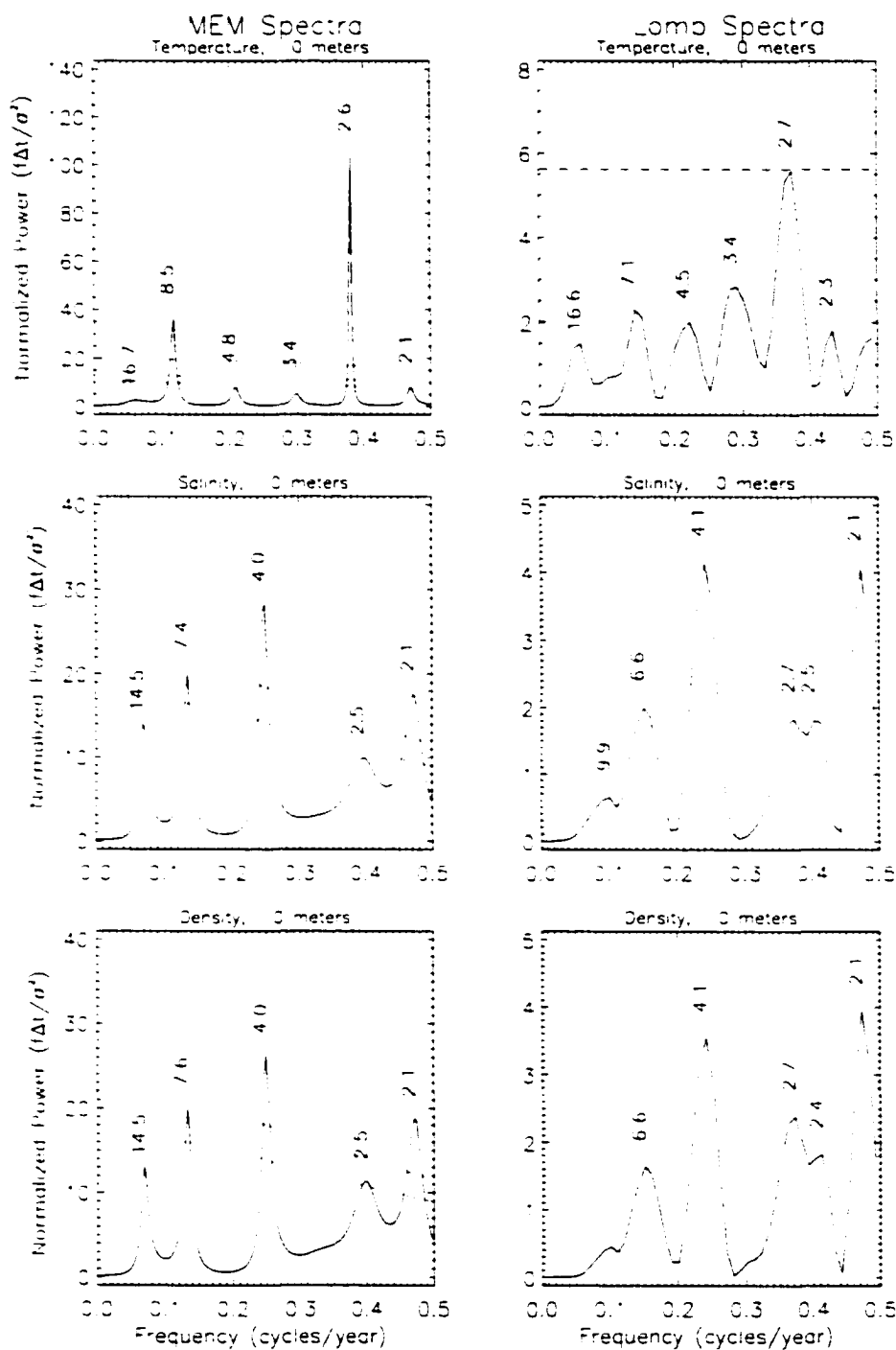


Figure 6: Spectral analyses of hydrographic parameters at 0 m depth. For all of figures 6 through 14, the 90%, 95% and 99% confidence intervals have been marked on the MEM spectra while the Lomb spectra show 95% and 99% confidence intervals. The periods of the peaks has been indicated in years.

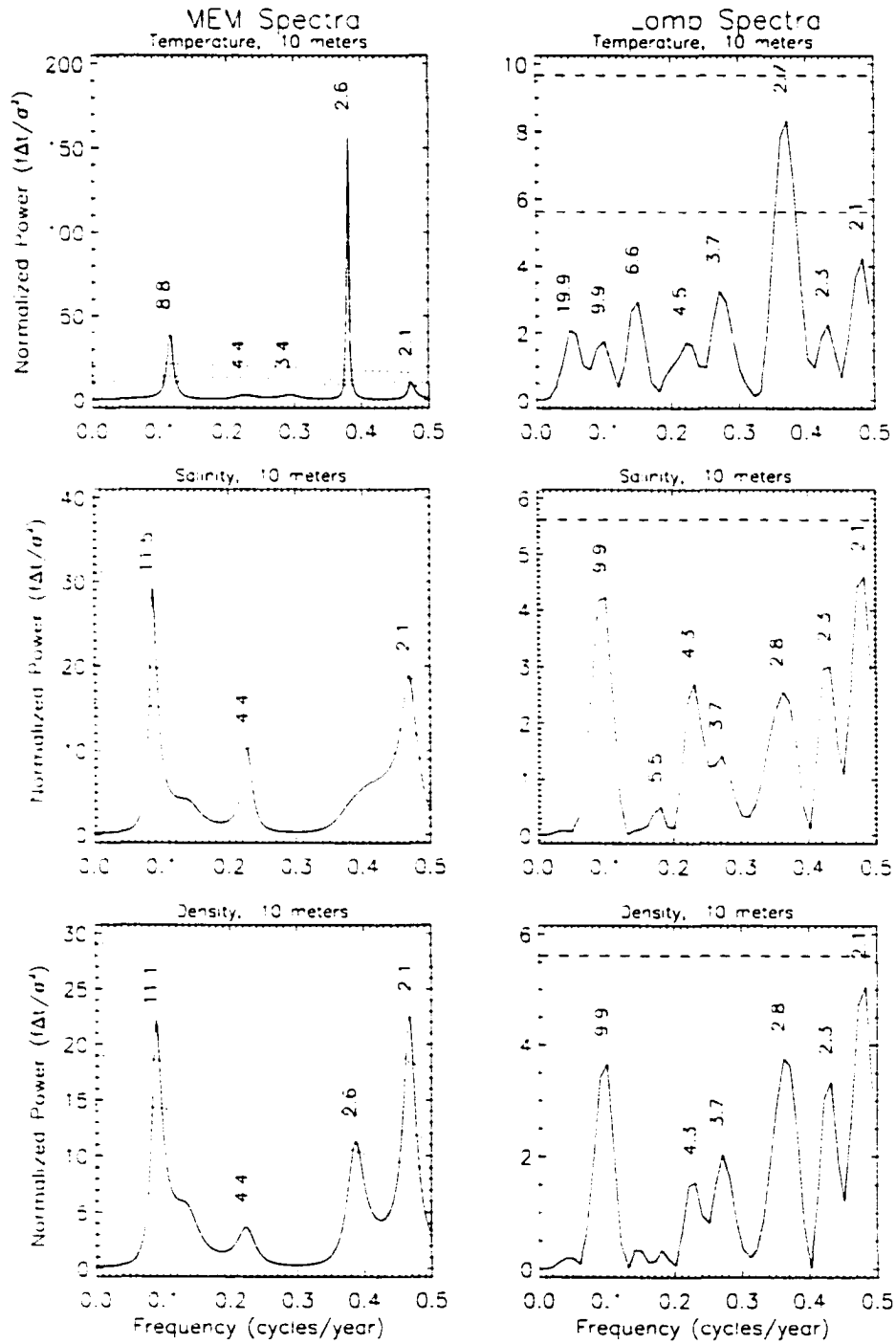


Figure 7: Spectral analyses of hydrographic parameters at 10 m depth.

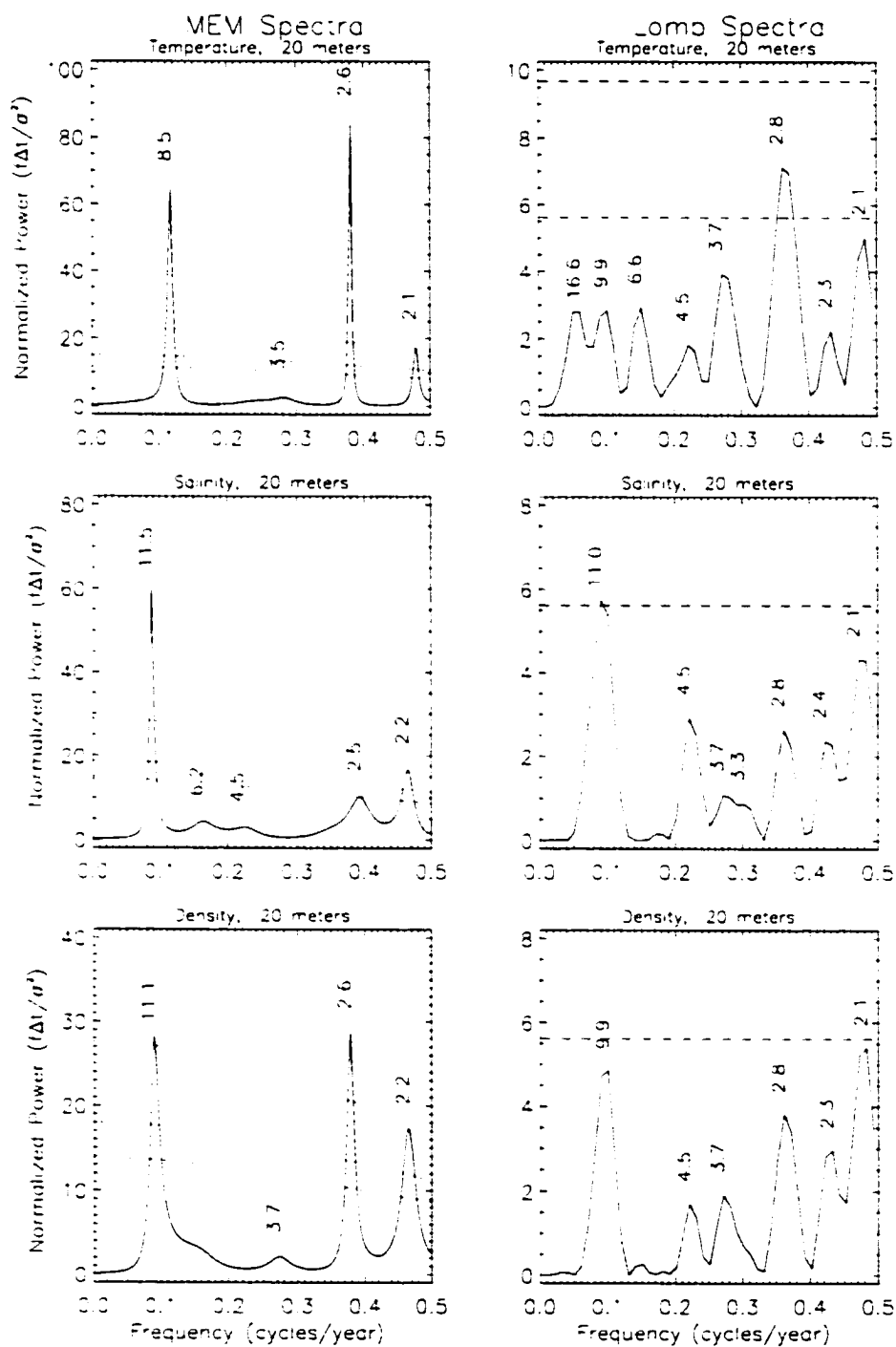


Figure 8: Spectral analyses of hydrographic parameters at 20 m depth.

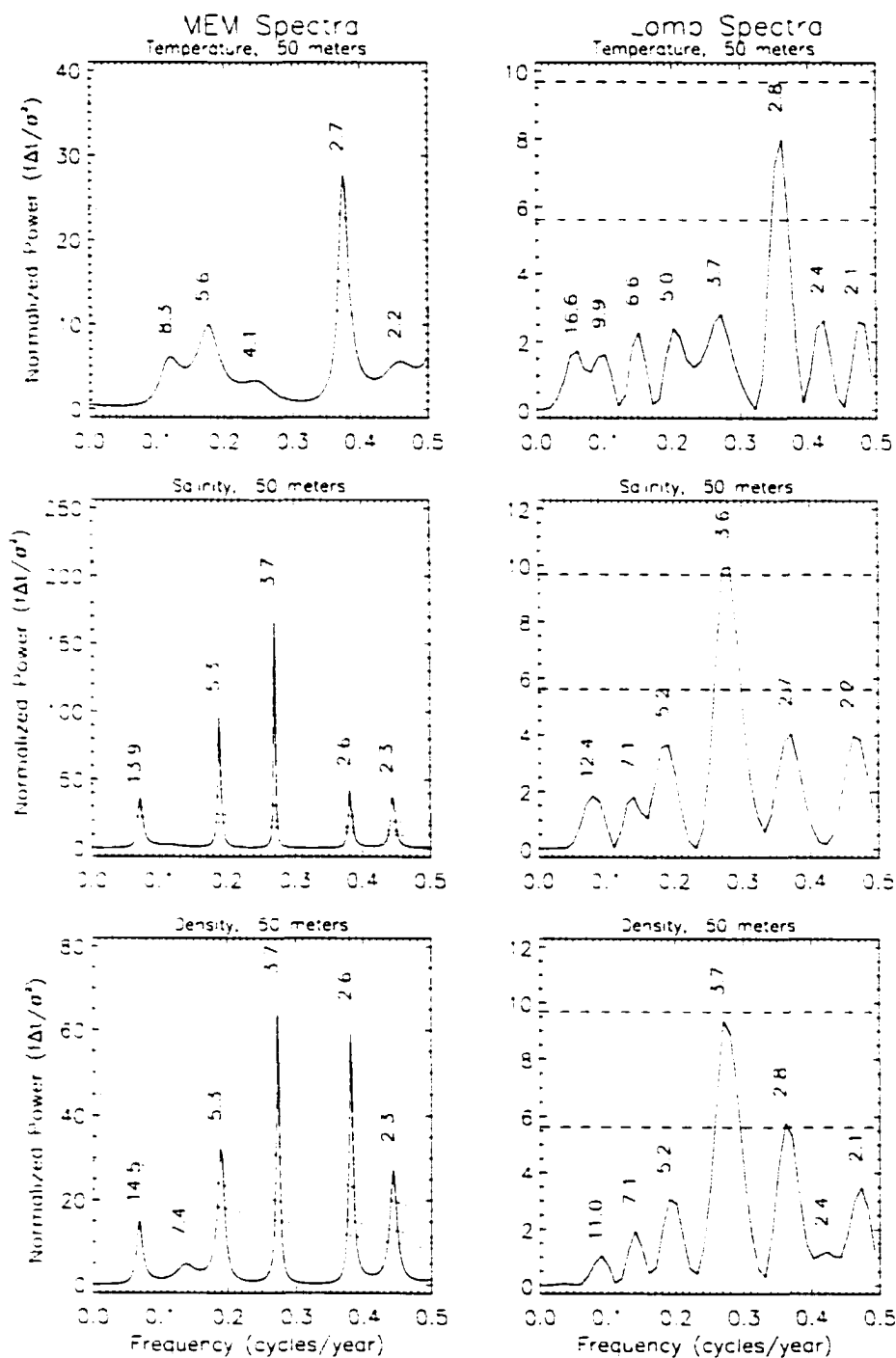


Figure 9: Spectral analyses of hydrographic parameters at 50 m depth.

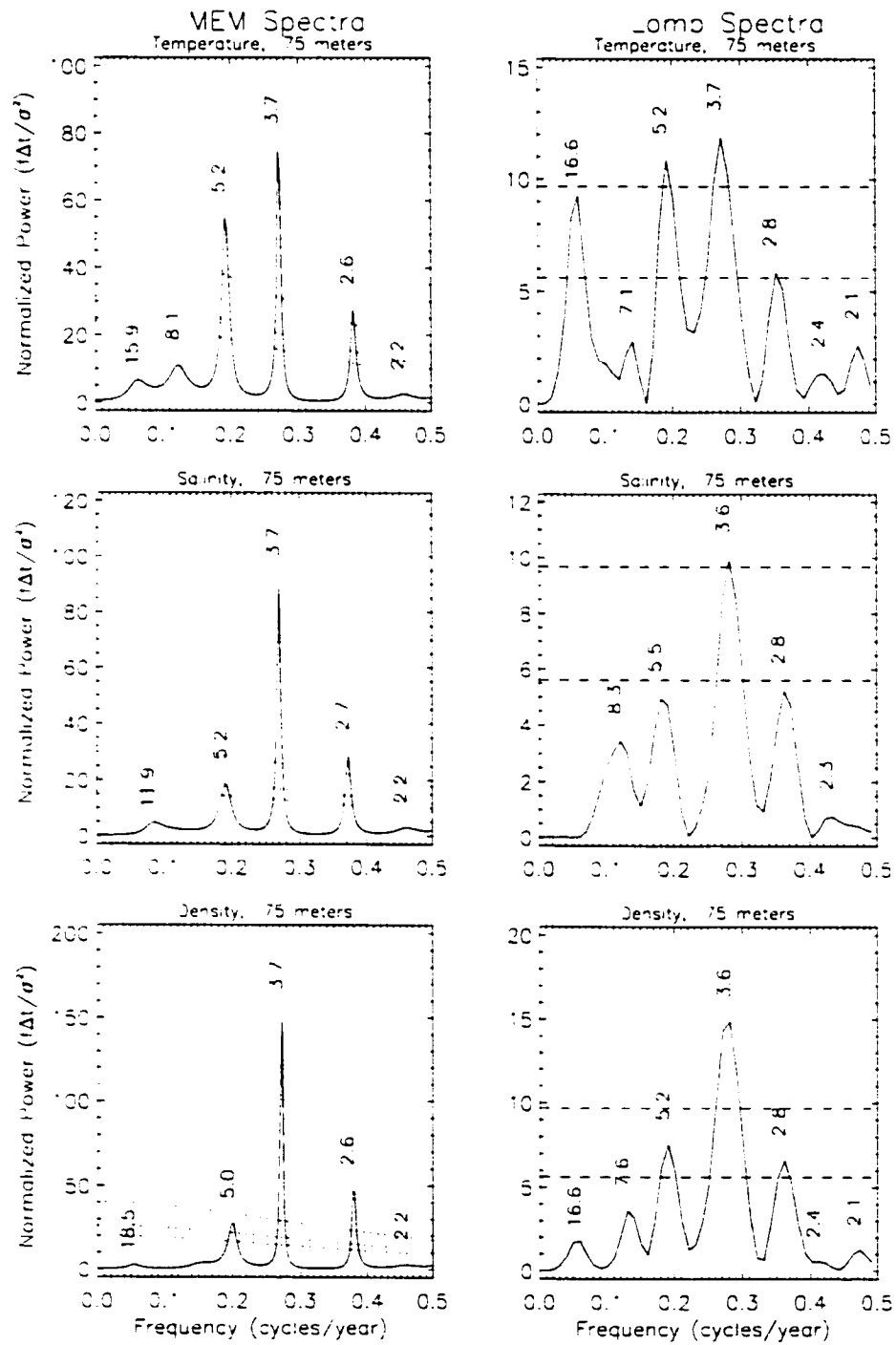


Figure 10: Spectral analyses of hydrographic parameters at 75 m depth.

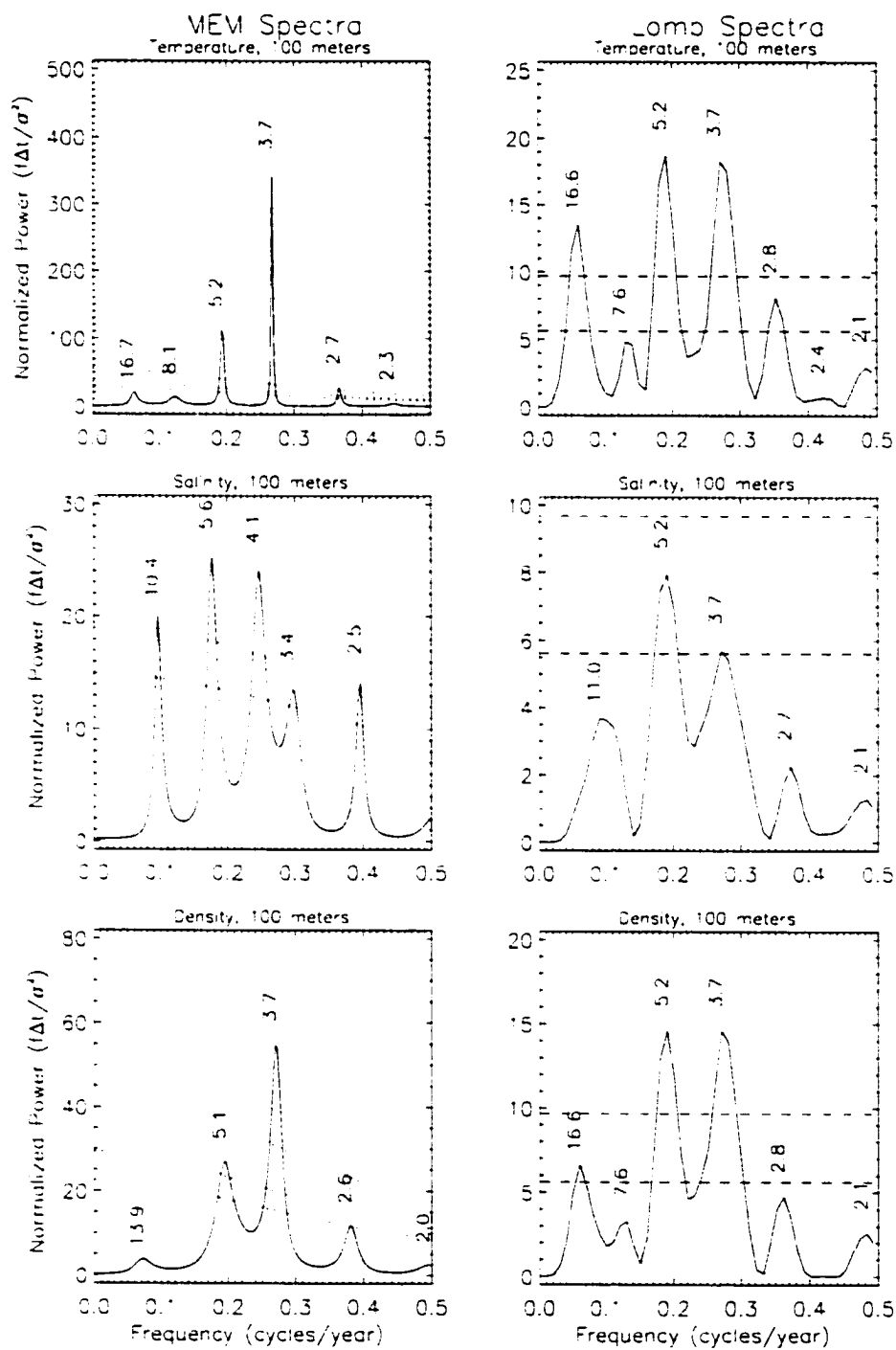


Figure 11: Spectral analyses of hydrographic parameters at 100 m depth.

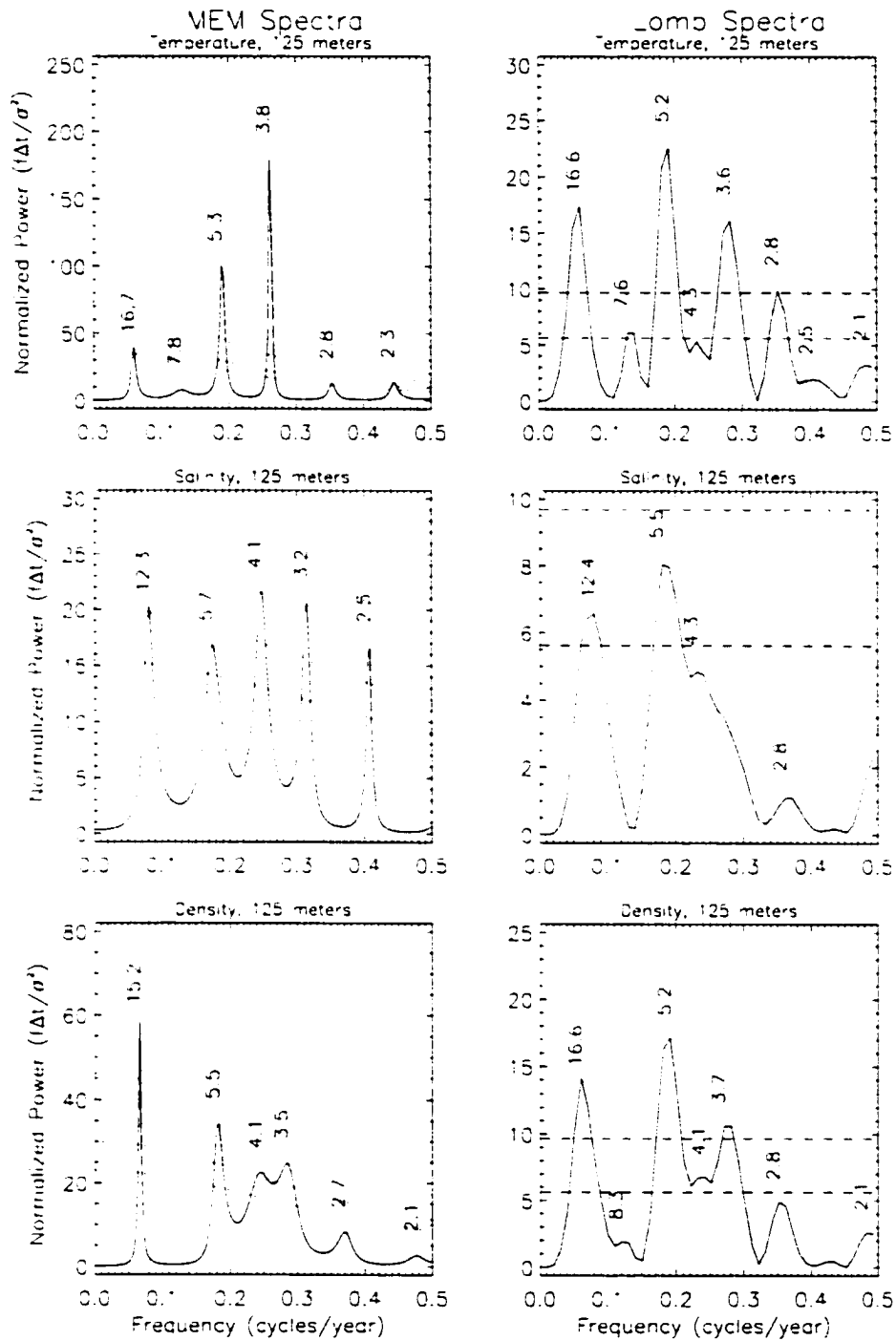


Figure 12: Spectral analyses of hydrographic parameters at 125 m depth.

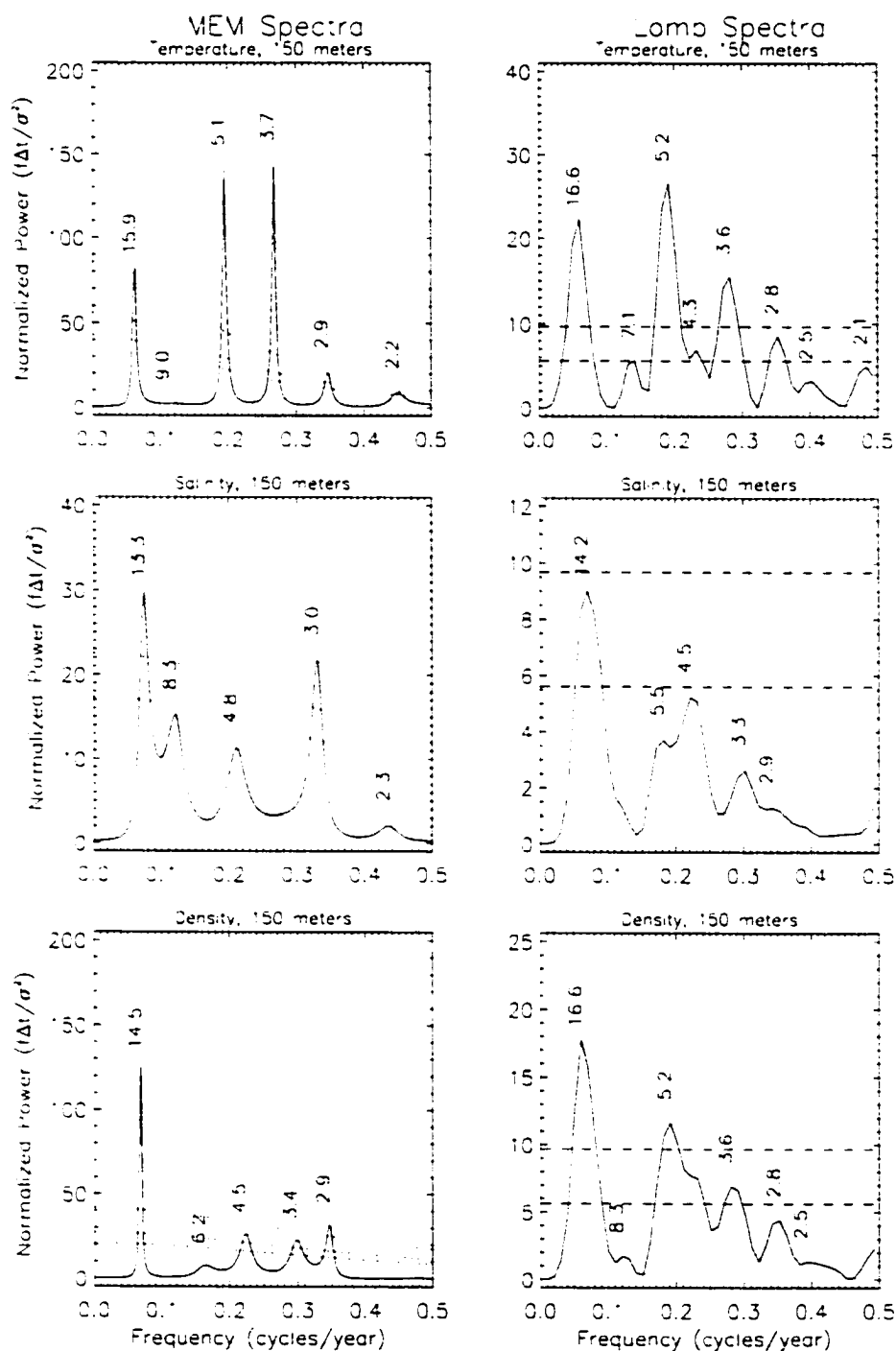


Figure 13: Spectral analyses of hydrographic parameters at 150 m depth.

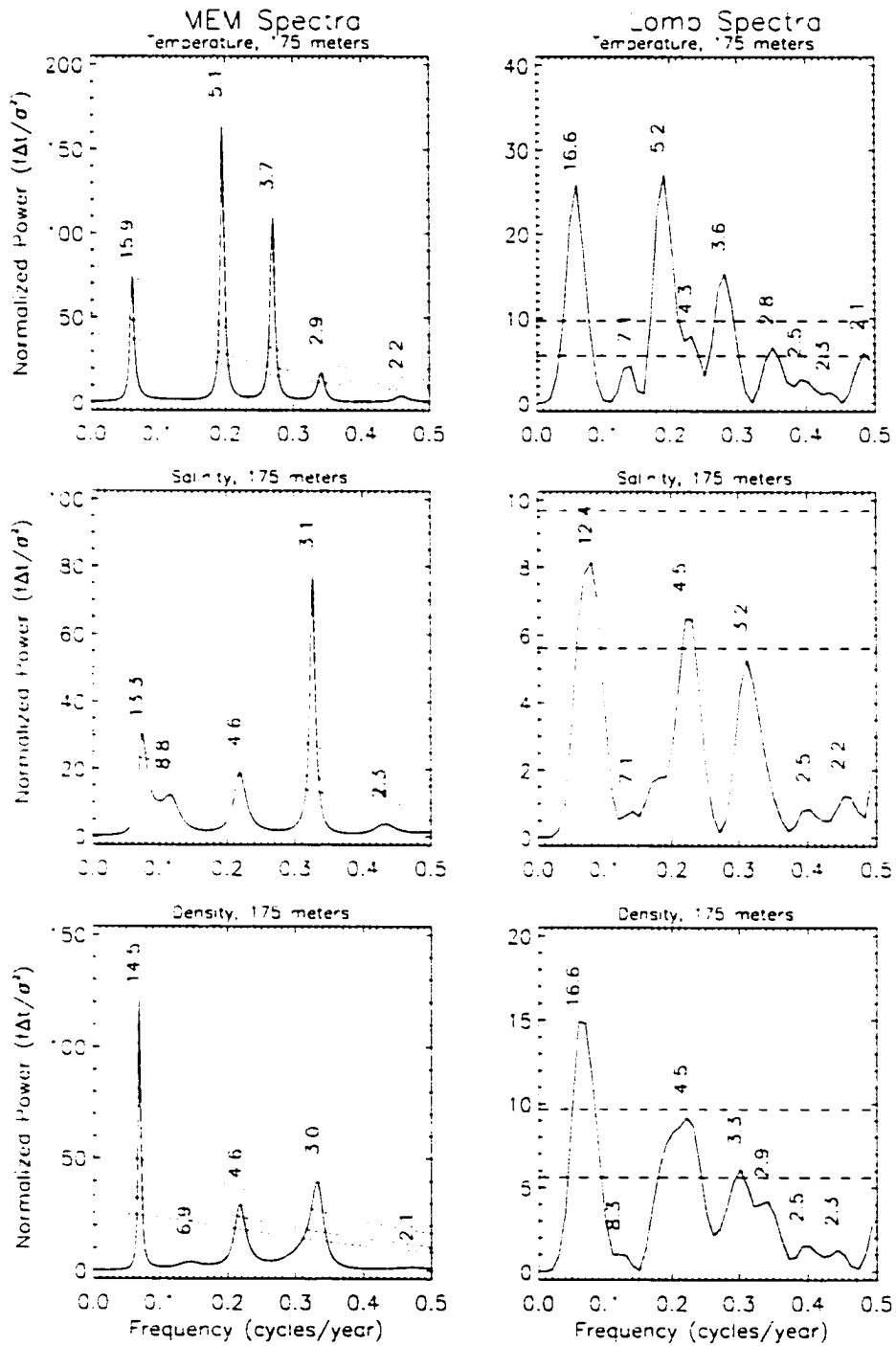


Figure 14: Spectral analyses of hydrographic parameters at 175 m depth.

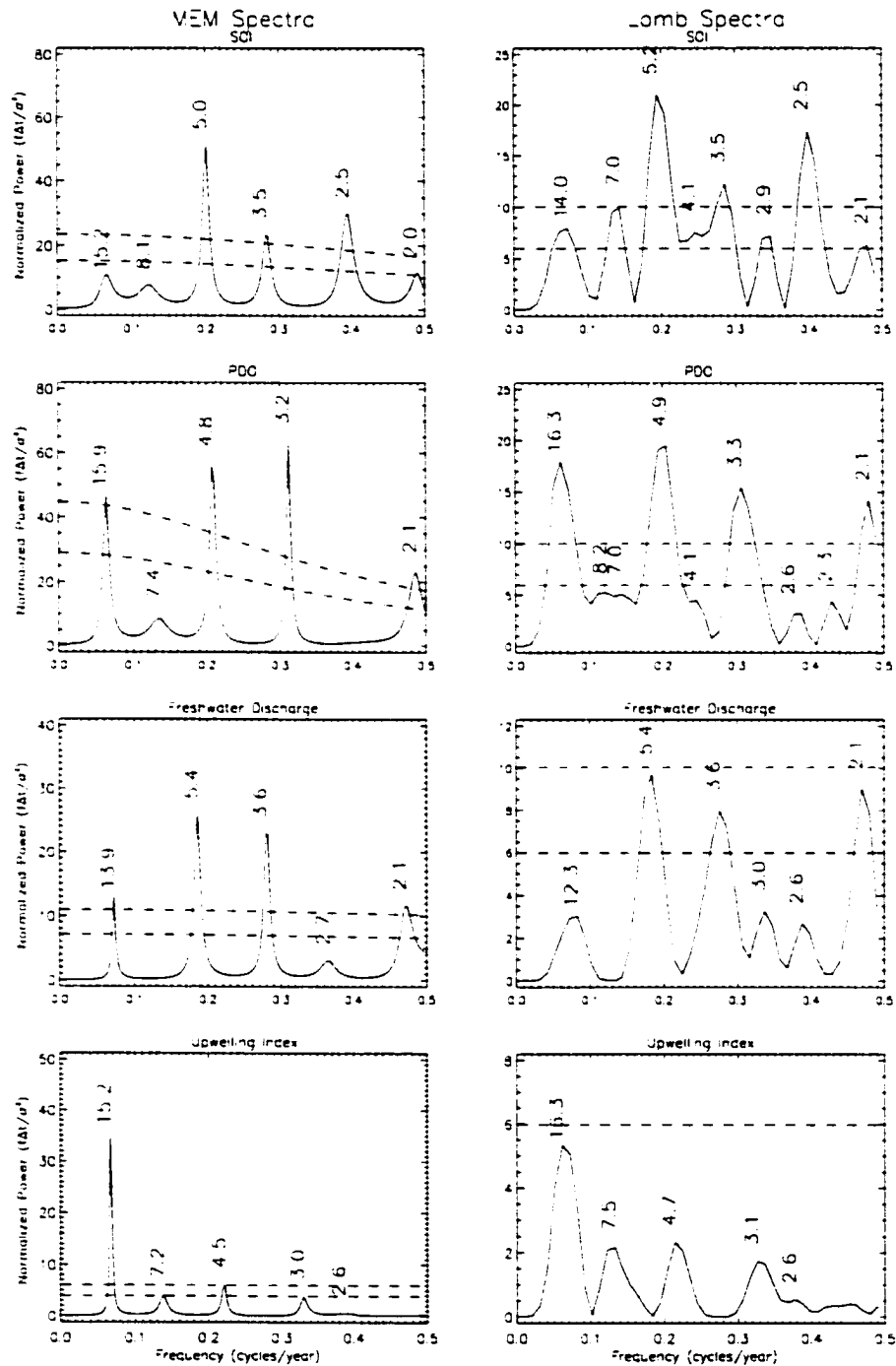


Figure 15: Spectral analysis of selected environmental parameters between 1974 and 1998. The 95% and 99% confidence intervals have been marked on the MEM and the Lomb spectra. The periods of the peaks has been indicated in years.

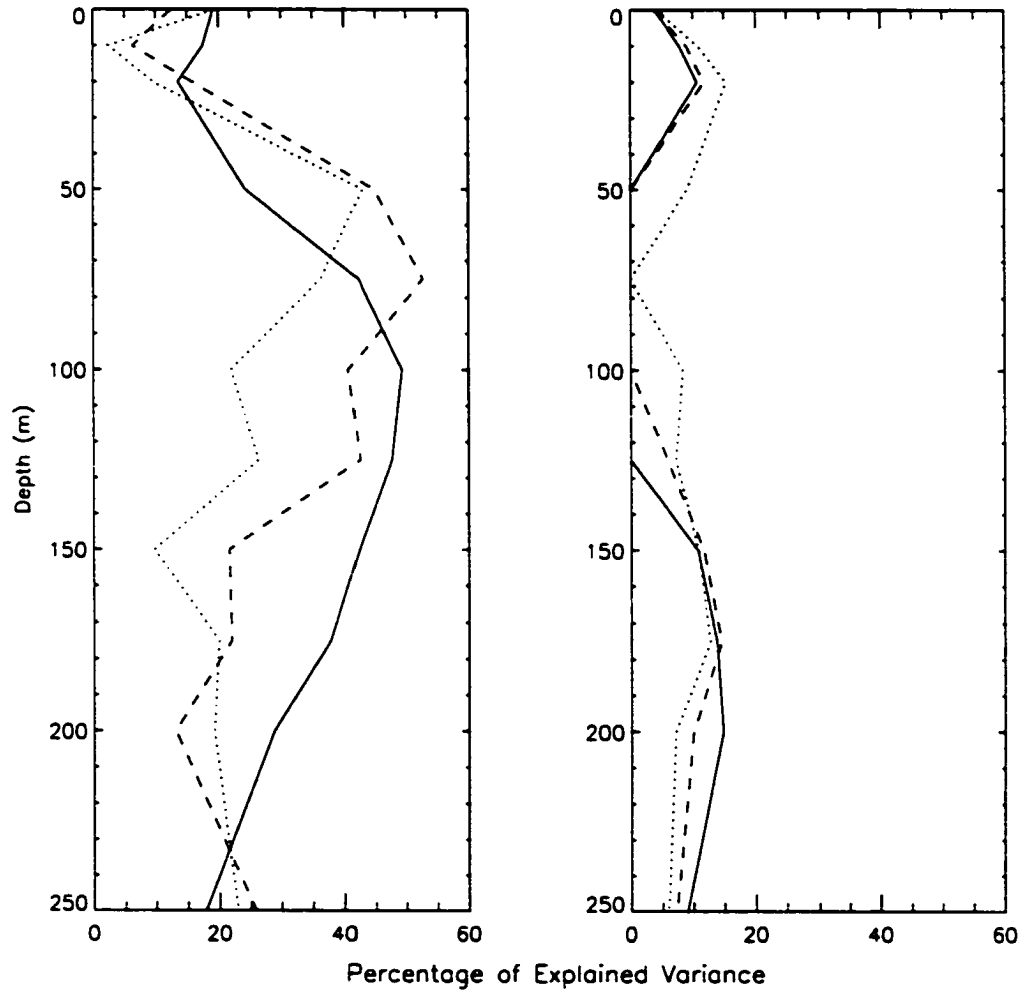


Figure 16: Explained variances of (a) ENSO (2-7 years) and (b) Decadal (10-18 years) periodicities in temperature (solid line), salinity (dotted line) and density (dashed line)

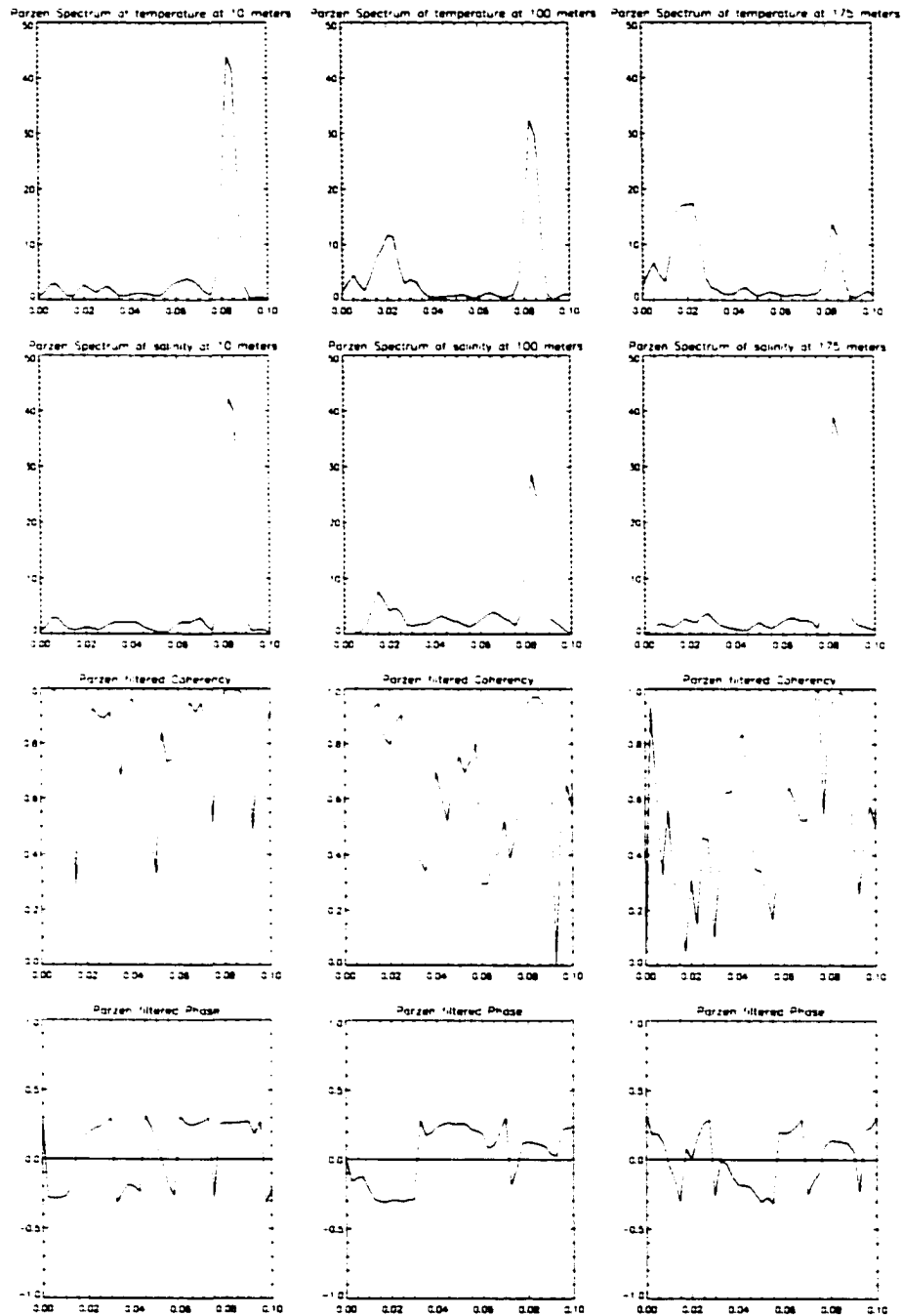


Figure 17: Cross-spectral analysis of temperature and salinity at 10 m, 100 m and 175 m. The spectra are normalized and the frequency is in units of *cycles/month*. The phase has been normalized by π .

Chapter 5

Conclusions

For this coastal site in the northern Gulf of Alaska, there is an annual cycle of MLD that varies seasonally from 40 m to 155 m. This has special biological significance for production by bringing deep nutrients into the surface layers. Deepening winter MLDs is likely a mechanism that supports primary production in the region, since the source of upper layer nutrients is the deep water.

There is a controversy regarding the mechanism by which nutrients reach the northern shelf of the GOA. Several pathways have been proposed for the transport of nutrients across the GOA northern shelf. The possible pathways are:

- 1) near surface cross-shelf transport by winds,
- 2) cross-shelf transport near bottom, especially within canyons, and
- 3) cross-shelf transport by mesoscale eddies.

One scenario is that the deep, nutrient-rich waters from the central Gulf of Alaska are brought onto the shelf from the open ocean within canyons. However, once the nutrients are brought onto the shelf, they need to be brought into the euphotic zone to be made available for biological production. I suggest that the MLDs in the northern Gulf of Alaska are sufficiently deep to mix the nutrients from the deep waters into the surface layers. Thus the winter MLD would be very important to the vertical nutrient flux here, and hence the biological productivity.

Importantly, the MLDs at GAK 1 behave differently than the MLDs at OSP and the trend across the North Pacific is not uniform as previously assumed

[Polovina *et al.*, 1995]. At GAK 1, there is no significant trend, though there is a deepening between 50-100m/century as calculated by the algorithm and the two independent methodologies. This is in contrast to a significant shallowing trend at OSP of the rate of 63 m/century [Freeland *et al.*, 1997]. It is possible that there is an out of phase relationship in MLDs in the northern Pacific. The gyre system and the Aleutian Low in the North Pacific are dominant parts of the system. Winter MLDs could be shoaling at the center of the gyre (OSP) while they deepen at the edge of the gyre (GAK 1). This indicates consistent dynamics with opposite nutrient supply conditions at the edge of the gyre as compared to the center of the gyre. The maximum MLD at GAK 1 also appears to be controlled by the regional factors of upwelling and freshwater discharge rather than by global factors like SOI and PDO. This appears to be a special characteristic of GAK 1 due to its coastal location near sources of freshwater discharge and in a predominantly downwelling regime. However, ENSO might influence the pycnocline and hence MLDs.

The spectra of water density at GAK 1 do not reflect solely either the temperature spectra or the salinity spectra, but a combination of the two. The temperature and density spectra are most similar at a depth of 100 m. This is in spite of the fact that salinity has a greater influence on density than temperature throughout the year and at all depths. Although temperature and salinity are independent variables, there is a definite correlation between them due to the association of these properties in water-masses. In addition, the range of temperature is much higher than the range of salinity. These factors together produce a combined effect of temperature and salinity spectra on the density spectra. It is possible that they work together with cold, salty water increasing the density and warm, fresh water decreasing it. Thus the influences of each are additive, leading to significant density variations.

Spectral analysis of the environmental parameters as time series from 1974-1998 show that SOI has ENSO frequencies and PDO has a bi-decadal frequency along with ENSO-like periodicities. The upwelling index is dominated by the bi-decadal frequency while freshwater discharge consists primarily of the ENSO-like

periodicities and the bidecadal periodicity to a lesser degree. It is evident that the effect of regional temperature and pressure patterns like SOI and PDO are remote signals and are linked indirectly to the hydrography through freshwater discharge and upwelling. Another teleconnection of the ENSO signal to the hydrography is as a Kelvin wave propagating along the shelf break [Meyers et al., 1998]. It has also been suggested that the hydrography of the region may be more closely linked to the extra-tropical Northern Oscillation Index (NOIx) [Schwing et al., 2000]. NOIx is a measure of the extra-tropical basin-wide atmospheric pressure variation, centered off California.

Since MLDs are related to mixing of the water column which in turn is related to nutrient supply and new production, information on the variation of 'N' (buoyancy frequency) with depth and season may be important. *Denman and Gargett* [1988] found that a step in the temperature profile above the seasonal thermocline at OSP is evident in the 'N' profile too, and separates the mixed layer into different bio-optical regimes. MLDs at GAK 1 could be calculated from such 'N' profiles, especially as advection decreases the reliability of other methods. Fitting of a step function to the depth profile of the buoyancy frequency should give closer estimates to the true value of the MLD.

Future work in the region needs to include analysis of MLDs along the Seward line in the Gulf of Alaska, possibly by using the Price, Weller and Pinkel (PWP) model [Price et al., 1986]. The PWP model is a one dimensional bulk model. Originally used for diurnal cycles, this model computes the mixed layer depth by including the competing effects of surface heating and wind stress. The Mathieu and deYoung modifications [Mathieu and deYoung, 1995] will be required to include the effect of salinity in the density calculations and to include diffusion terms. These terms will be important for timescales of the order of years. Additional advection terms also need to be added in the equation for the conservation of salt. Finally, this model should be coupled to a nutrient model to verify that the deepening of the seasonal MLD could be the mechanism that is responsible for bringing nutrients up into the euphotic zone.

The results of this study demonstrate the out of phase relationship of the seasonal MLDs at the center and the periphery of the North Pacific gyre system. The depths of the seasonal MLD also provide a plausible explanation for the mechanism that mixes nutrients into the euphotic zone and thus supports biological activity in the region. in contrast to the hypothesis of the nutrients being advected onto the shelf in the upper wind driven layers.

References

- Bakun, A.. Coastal upwelling indices, west coast of North America, 1946-71. *Tech. Rep. NMFS SSRF-671*. NOAA, 1973.
- Beamish, R. J., and D. R. Bouillon. Pacific salmon trends in relation to climate. *Can. J. Fish. Aquat. Sci.*, 50, 1002-1016, 1993.
- Bjerknes, J.. Atmospheric teleconnections from the equatorial Pacific. *Mon. Weather Rev.*, 97, 163-172, 1969.
- Brodeur, R. D., and D. M. Ware. Long-term variability in zooplankton biomass in the subarctic Pacific Ocean. *Fish. Oceanogr.*, 1, 32-38, 1992.
- Denman, K., and A. E. Gargett. Multiple thermoclines are barriers to vertical exchange in the subarctic Pacific during SUPER. May 1984. *J. Mar. Res.*, 46, 77-103, 1988.
- Emery, W. J., and R. E. Thomson. *Data Analysis Methods in Physical Oceanography*. Pergamon Press, New York, USA, 1998.
- Eppley, R. W., and B. J. Peterson. Particulate organic matter flux and planktonic new production in the deep ocean. *Nature*, 282, 677-680, 1979.
- Fofonoff, N. P.. Physical properties of seawater: a new salinity scale and equation of state for seawater. *J. Geophys. Res.*, 90, 3332-3342, 1985.
- Freeland, H., and F. Whitney. Climatic changes: Gulf of Alaska. in *Seas at the millennium : an environmental evaluation*, edited by C. R. C. Sheppard, pp. 395-414, Pergamon, Amsterdam, 2000.
- Freeland, H., K. Denman, C. S. Wong, F. Whitney, and R. Jacques. Evidence of change in the winter mixed layer in the northeast Pacific Ocean. *Deep Sea Res.*, 44, 2117-2129, 1997.
- Gargett, A. E.. The optimal stability 'window': a mechanism underlying fluctuations in the north Pacific salmon stocks?. *Fish. Oceanogr.*, 6, 109-117, 1997.

- Gargett, A. E., M. Li, and R. Brown. Testing mechanistic explanations of observed correlations between environmental factors and marine fisheries, *Can. J. Fish. Aquat. Sci.*, *58*, 208–219, 2001.
- Hare, S. R., N. J. Mantua, and R. C. Francis. Inverse production regimes: Alaska and west coast Pacific salmon. *Fish.*, *24*, 6–14, 1999.
- Jaynes, E. T., Prior probabilities, *IEEE Trans. Sys. Sci. Cybern.*, *SEC-4*, 227–241, 1968.
- Kendall, M., and J. D. Gibbons. *Rank Correlation Methods*, Edward Arnold, New York, USA, 1990.
- Latif, M., and N. E. Graham. How much predictive skill is contained in the thermal structure of an OGCM?, *J. Phy. Oceanogr.*, *22*, 951–962, 1992.
- Lawson, P. W., Cycles in ocean productivity, trends in habitat quality, and the restoration of salmon runs in Oregon. *Fish.*, *18*, 6–10, 1993.
- Lomb, N. R., Least-squares frequency-analysis of unequally spaced data, *Astrophys. Space Sci.*, *39*, 447–462, 1976.
- Mann, K., and J. Lazier. *Dynamics of Marine Ecosystems*, 2nd ed., Blackwell Science, Inc., Cambridge, USA, 1996.
- Mann, K. H., Physical oceanography, food chains and fish stocks: a review, *ICES J. Mar. Sci.*, *50*, 105–119, 1993.
- Mantua, N. J., S. R. Hare, Y. Zhang, J. M. Wallace, and R. C. Francis. A Pacific interdecadal climate oscillation with impacts on salmon production, *Bull. Am. Meteorol. Soc.*, *78*, 1069–1079, 1997.
- Mathieu, T., and B. deYoung. Application of a mixed layer model to the inner Newfoundland shelf, *J. Geophys. Res.*, *100*, 921–936, 1995.

- McFarlane, G., and R. J. Beamish, Climatic influence linking copepod production with strong year-classes in sablefish, *anoplopoma fimbria*, *Can. J. Fish. Aquat. Sci.*, *49*, 743–753, 1992.
- Meier, M. F., Contribution of small glaciers in global sea level, *Science*, *226*, 1418–1421, 1984.
- Meyers, S. D., A. Melsom, G. T. Mitchum, and J. J. O'Brien, Detection of the fast Kelvin wave teleconnection due to El-Niño-Southern Oscillation, *J. Geophys. Res.*, *103*, 27,655–27,663, 1998.
- Namias, J., Seasonal interactions between the north Pacific Ocean and the atmosphere during the 1960s, *Mon. Weather Rev.*, *97*, 173–192, 1969.
- Namias, J., Multiple causes of the North American abnormal winter 1976–77, *Mon. Weather Rev.*, *106*, 279–295, 1978.
- Navarra, A., *Beyond El Niño: Decadal and Interdecadal Climate Variability*, Springer-Verlag, Berlin, 1999.
- Neelin, J. D., D. S. Battisti, A. C. Hirst, F. F. Jin, Y. Wakata, T. Yagamata, and S. E. Zebiak, ENSO theory, *J. Geophys. Res.*, *103*, 14,261–14,290, 1998.
- Polovina, J. J., G. T. Mitchum, N. E. Graham, M. P. Craig, E. E. DeMartini, and E. N. Flint, Physical and biological consequences of a climate event in the central North Pacific, *Fish. Oceanogr.*, *3*, 15–21, 1994.
- Polovina, J. J., G. T. Mitchum, and G. T. Evans, Decadal and basin-scale variation in mixed alger depth and the impact on biological production in the central and north Pacific, *Deep Sea Res.*, *42*, 1701–1716, 1995.
- Price, J. F., R. A. Weller, and R. Pinkel, Diurnal cycling: observations and models of the upper ocean response to diurnal heating, cooling and wind mixing, *J. Geophys. Res.*, *89*, 8411–8427, 1986.
- Priestly, M. B., *Spectral Analysis and Time Series*, Academic Press, London, 1981.

- Rasmusson, E. M., X. Wang, and C. F. Ropelewski. The biennial component of ENSO variability. *J. Mar. Syst.*, *1*, 71–96, 1990.
- Reed, R. K., and W. P. Elliott. New precipitation maps for the North Atlantic and North Pacific Oceans. *J. Geophys. Res.*, *84*, 7839–7846, 1979.
- Royer, T. C.. Seasonal variations of waters in the northern Gulf of Alaska. *Deep Sea Res.*, *22*, 403–416, 1975.
- Royer, T. C.. On the effect of precipitation and runoff on coastal circulation in the Gulf of Alaska. *J. Phy. Oceanogr.*, *9*, 555–563, 1979.
- Royer, T. C.. Baroclinic transport in the Gulf of Alaska. II. A fresh water driven coastal current. *J. Mar. Res.*, *39*, 251–266, 1981.
- Royer, T. C.. Coastal freshwater discharge in the northeast Pacific. *J. Geophys. Res.*, *87*, 2017–2021, 1982.
- Royer, T. C.. Coastal processes in the northern North Pacific. in *The Sea*, edited by A. R. Robinson and K. H. Brink, vol. 11, pp. 395–414, John Wiley and Sons, New York, 1998.
- Schumaker, J. D., and R. K. Reed. Coastal flow in the northwest Gulf of Alaska: the Kenai current. *J. Geophys. Res.*, *85*, 6680–6688, 1980.
- Schwing, F. B., T. Murphree, and P. Green. A climate index for the northeast Pacific. *Prog. Oceanogr.*, p. in review, 2000.
- Shannon, C. E.. A mathematical theory of communication. *Bell Syst. Tech. J.*, *27*, 379–423, 1948.
- Sprintall, J., and D. Roemmich. Characterizing the structure of the surface layer in the Pacific Ocean. *J. Geophys. Res.*, *104*, 23,297–23,311, 1999.
- Ulrych, T. J.. Maximum entropy power spectrum of truncated sinusoids. *J. Geophys. Res.*, *77*, 1396–1400, 1972.

- Ulrych, T. J., and T. N. Bishop. Maximum entropy spectral analysis and autoregressive decomposition, *Rev. Geophysics Space Phys.*, *13*, 183–200. 1975.
- UNESCO, Tenth report of the joint panel on oceanographic tables and standards. *Tech. Rep. 36*. UNESCO, Paris, France, 1981.
- Wilson, J. G., and J. E. Overland. Meteorology, in *The Gulf of Alaska Physical Environment and Biological Resources*, edited by D. W. Hood and S. T. Zimmerman. OCS Study MMS86-0095, pp. 31–54, Minerals Management Service. Springfield, VA. 1986.
- Xiong, Q., and T. C. Royer. Coastal temperature and salinity in the Northern Gulf of Alaska, 1970–1983. *J. Geophys. Res.*, *89*, 8,061–8,068. 1984.
- Zhang, Y., J. M. Wallace, and D. S. Battisti. ENSO-like interdecadal variability: 1900–93. *J. Climate*, *10*, 1004–1020. 1997.

Vita

Nandita Sarkar

Department of Ocean, Earth and Atmospheric Sciences

Old Dominion University

Norfolk, VA 23529

PERSONAL DATA

I was born on 20 June 1974 in New Delhi, India to Biswajit and Jyoti Sarkar.

EDUCATION

B.Sc. Geography, July 1996, S. P. College, Pune, India.

M.Sc. Geography, July 1998, University of Pune, Pune, India.

MS Oceanography, August 2001, Center for Coastal Physical Oceanography,

Department of Ocean, Earth and Atmospheric Sciences, Old Dominion University,

Norfolk, VA 23529, USA.

POSTERS

Sarkar, N. and Royer, T. C., Decadal Mixed Layer Depth Variability in the Northern Gulf of Alaska. AGU Ocean Sciences Meeting, San Antonio, TX.

February 2000.

MEMBERSHIPS

American Geophysical Union

Typeset using L^AT_EX.